



New Positron Beam Applications: Positrons Reveal Lattice Defects in Functional Materials and Electronic Structure in Correlated Systems

Christoph Hugenschmidt

Technische Universität München



New Positron Beam Applications: **Positrons Reveal Lattice Defects** in Functional Materials and **Electronic Structure** in Correlated Systems

Christoph Hugenschmidt

Technische Universität München

Positron Beam Facility at NEPOMUC



NEPOMUC

Positron Source
SR11

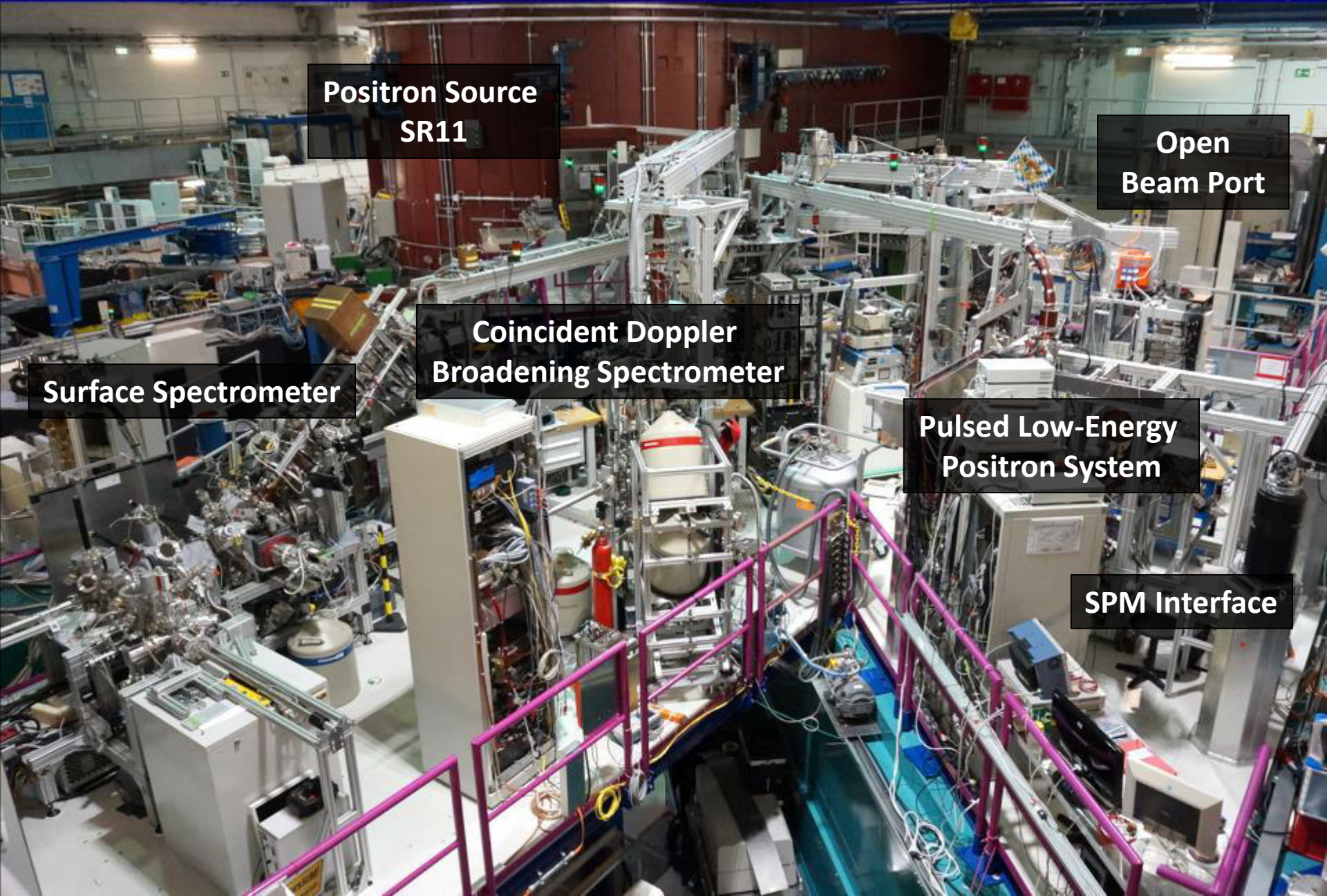
Open
Beam Port

Coincident Doppler
Broadening Spectrometer

Surface Spectrometer

Pulsed Low-Energy
Positron System

SPM Interface



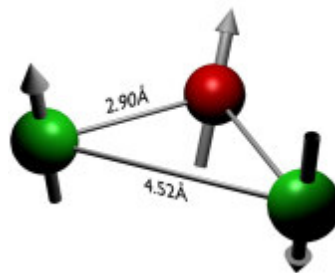
Positron Beam Facility at NEPOMUC



NEPOMUC

Positron Source
SR11

Fundamental Physics



H. Ceeh et al.
PRA 84 (2011) 062508



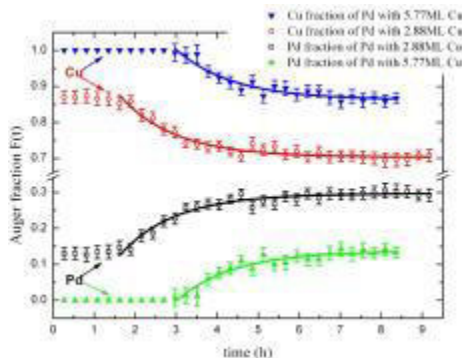
T. Sunn Pedersen et al.
New J. Phys. 14 (2012) 035010

Open
Beam Port

Coincident Doppler
Broadening Spectrometer

Surface Spectrometer

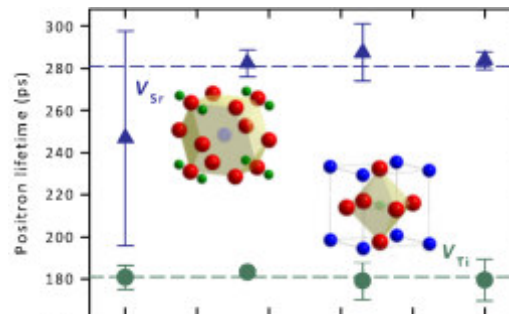
Positron Auger
Electron Spectroscopy



J. Mayer et al. PRL 05 (2010) 207401

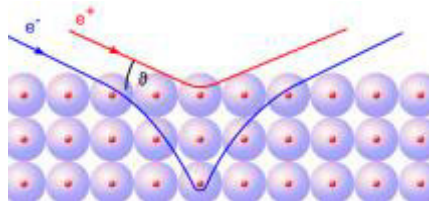
Pulsed Low-Energy
Positron System

Positron Lifetime Spectroscopy



D. Keeble et al. PRB 87 (2013) 195409

NEW: Positron Diffraction



C.H., Surf. Sci. Rep. 6 (2016) 547

Outline

Positrons in Matter

Part I

(C)DBS at NEPOMUC

YBCO

AlCu6Mn

Part II

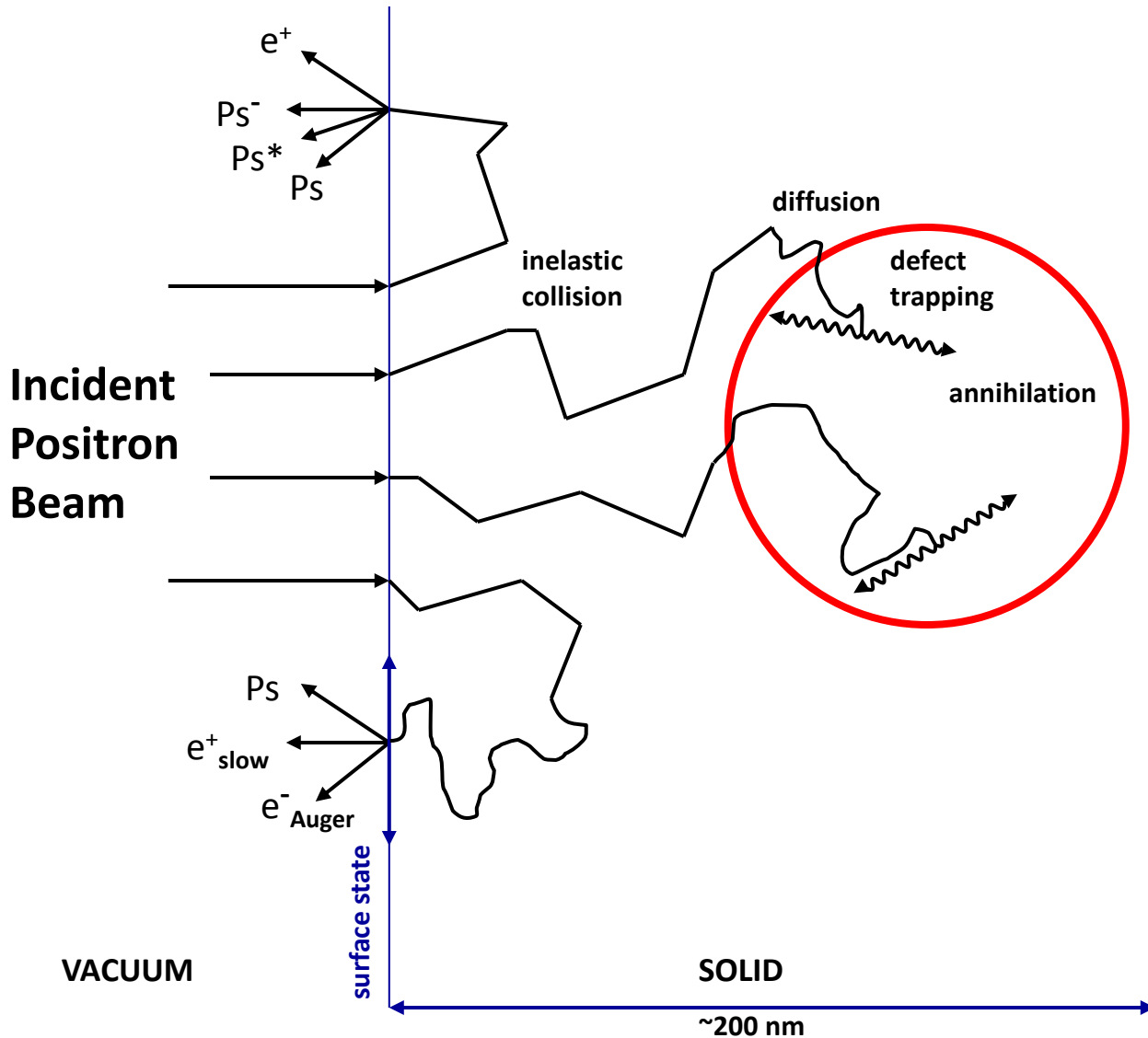
2D-ACAR with ^{22}Na

Ni

Cu_2MnAl

Conclusion & Future

Positrons in Matter



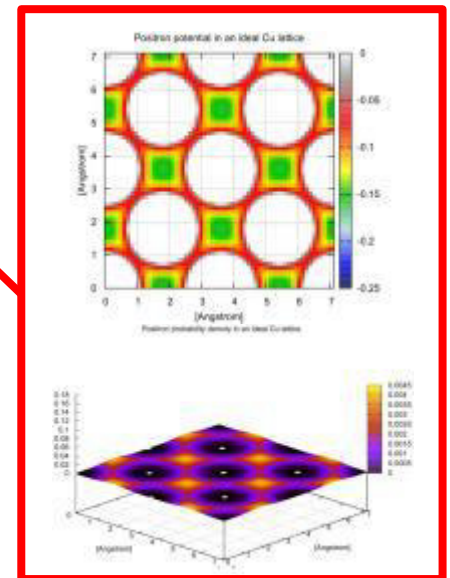
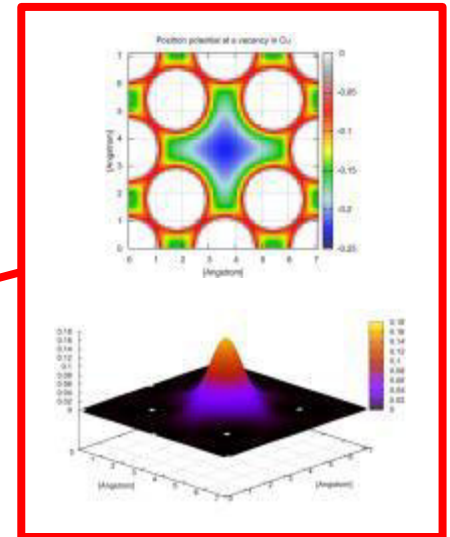
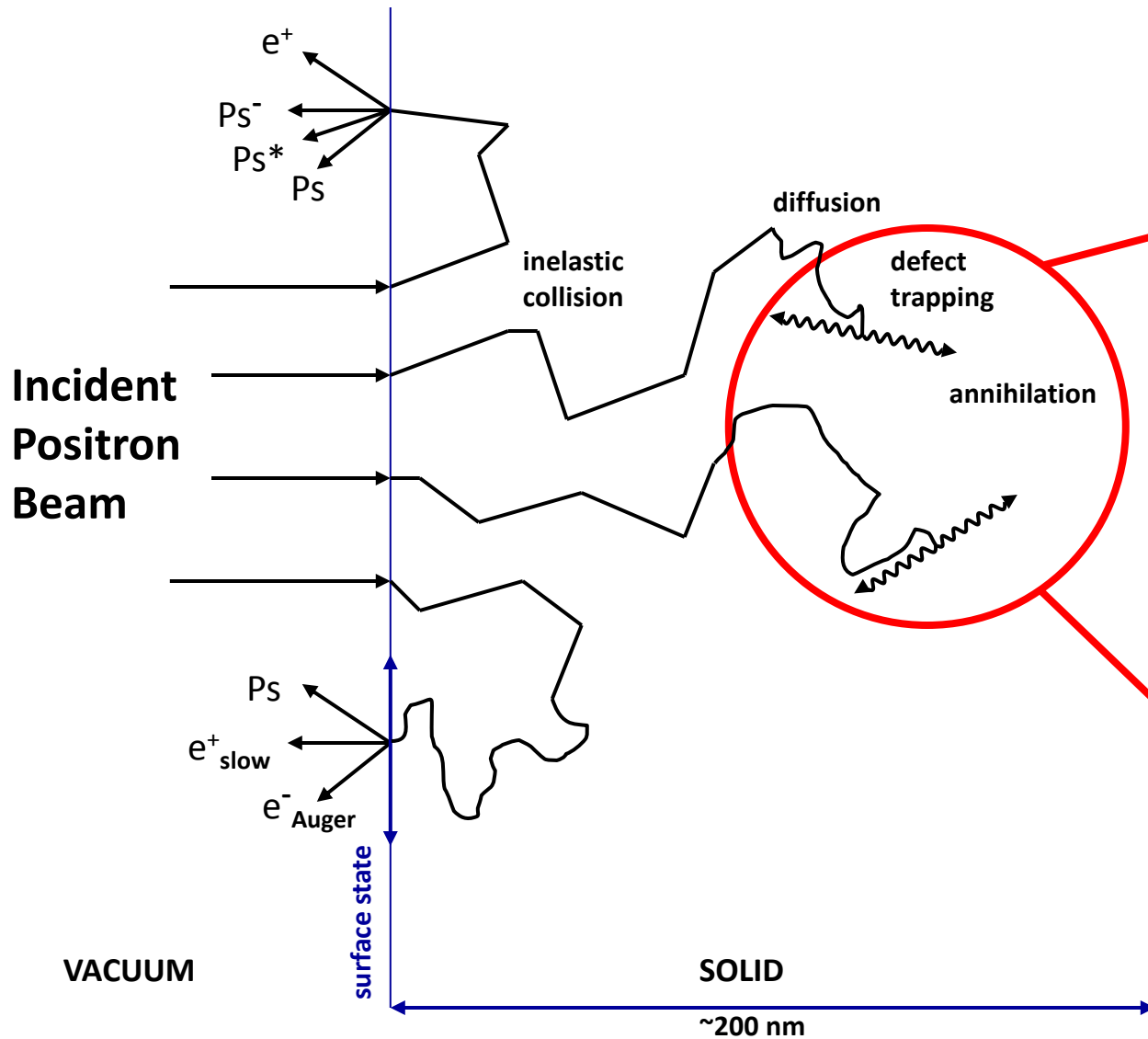
Positrons fate:

- thermalization
 $\sim 10^{-12}$ s
- diffusion
 $\sim 10^{-10}$ s
 $\rightarrow \sim 100$ nm
- defect trapping
- annihilation
 $\rightarrow 2$ collinear γ -quanta

Experiment:

- positron lifetime τ
 $\rightarrow \rho(e^-)$
- Doppler-broadening ΔE
Angular correlation $\Delta\Theta$
 $\rightarrow p(e^-)$
- Auger-electrons
 $\rightarrow E_b(e^-)$

Positrons in Matter

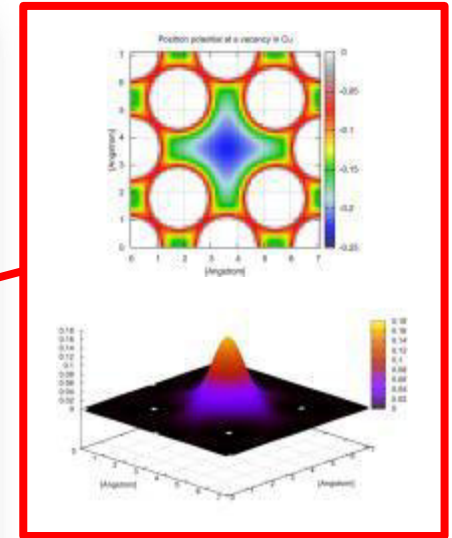
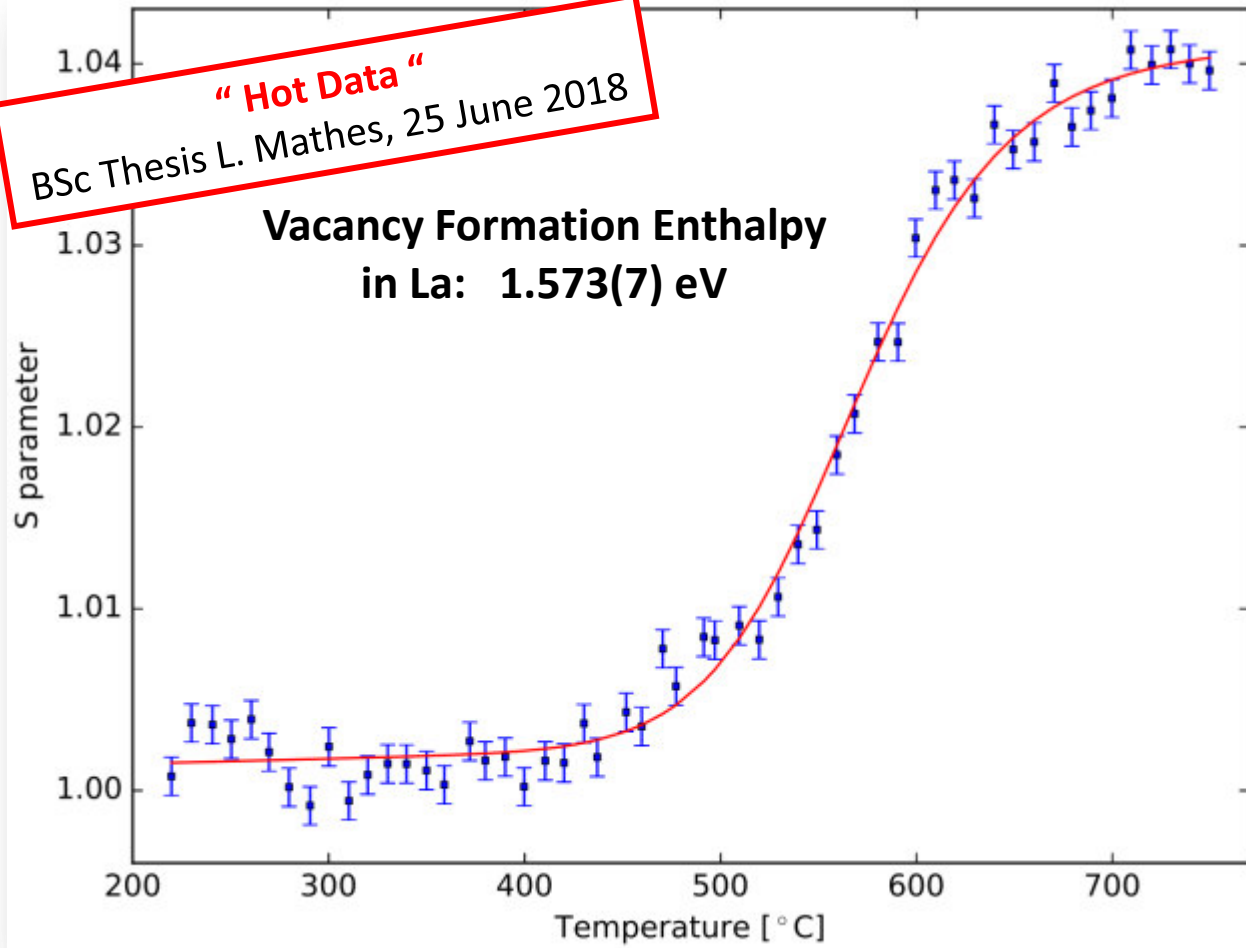


Positrons in Matter

“ Hot Data ”

BSc Thesis L. Mathes, 25 June 2018

**Vacancy Formation Enthalpy
in La: 1.573(7) eV**



VACUUM

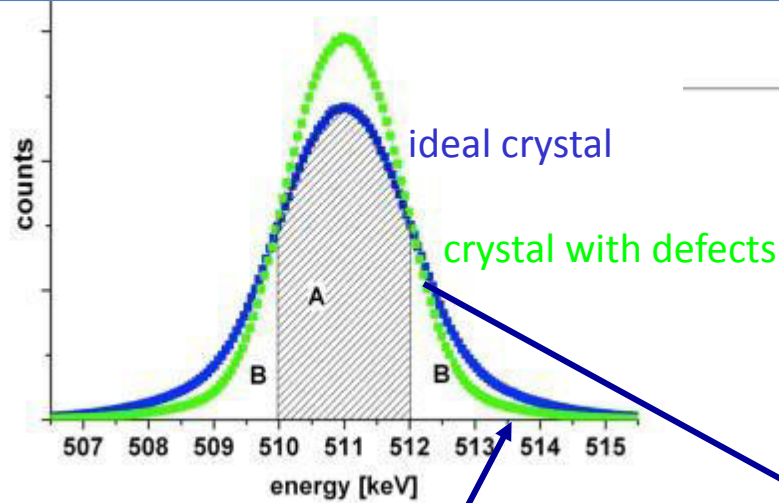
surface state

SOLID

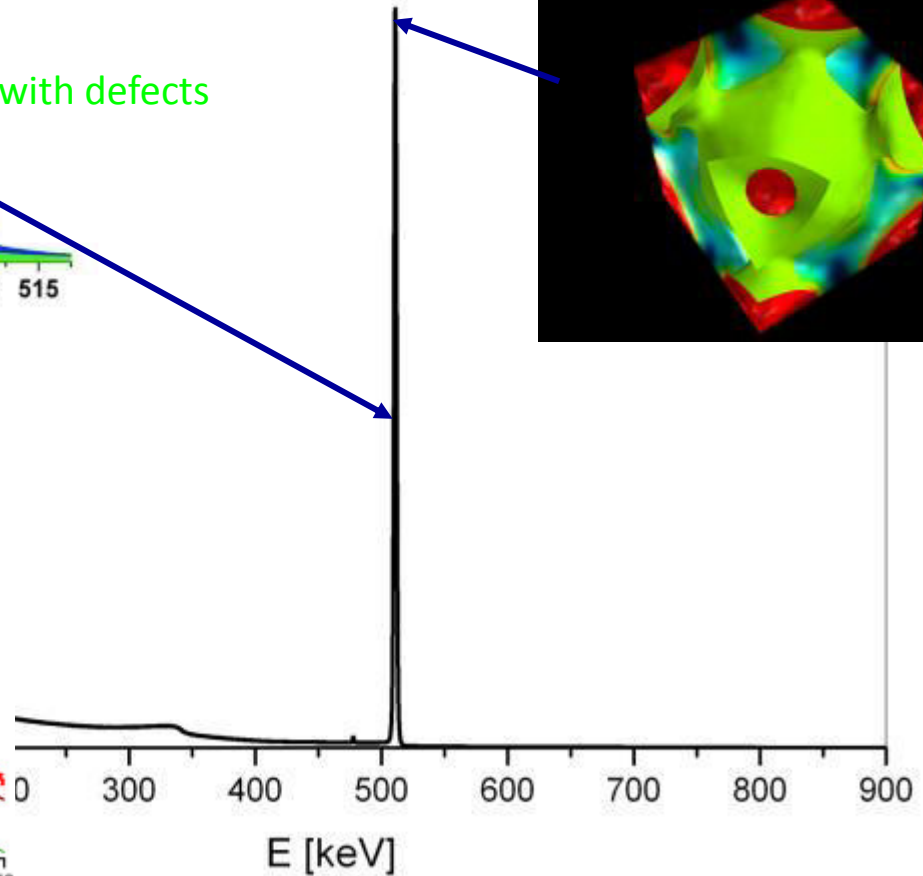
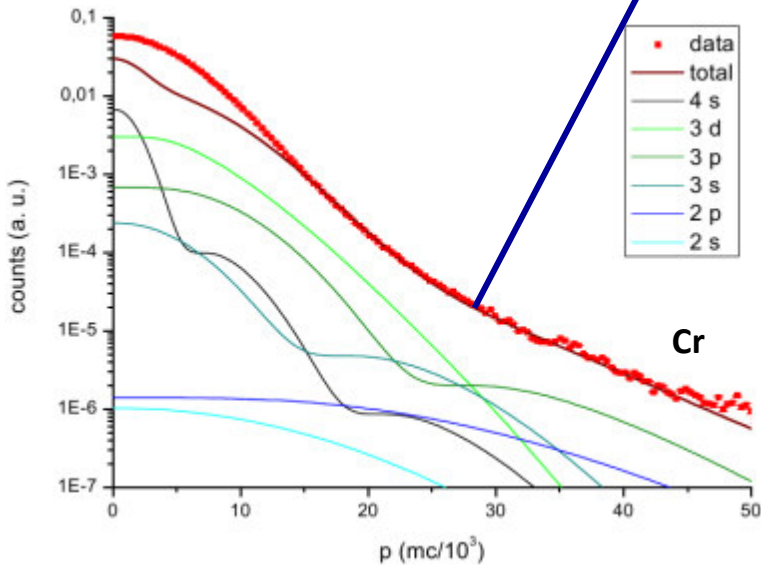
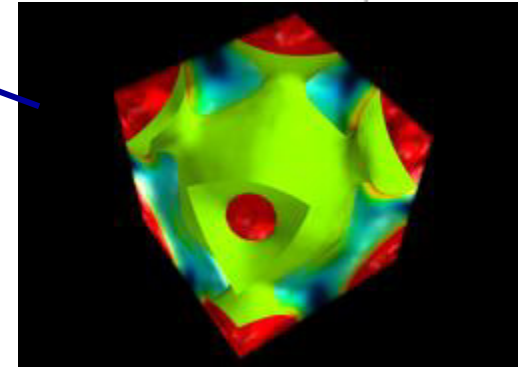
~200 nm

What We Measure

Doppler-Broadening Spectroscopy – DBS

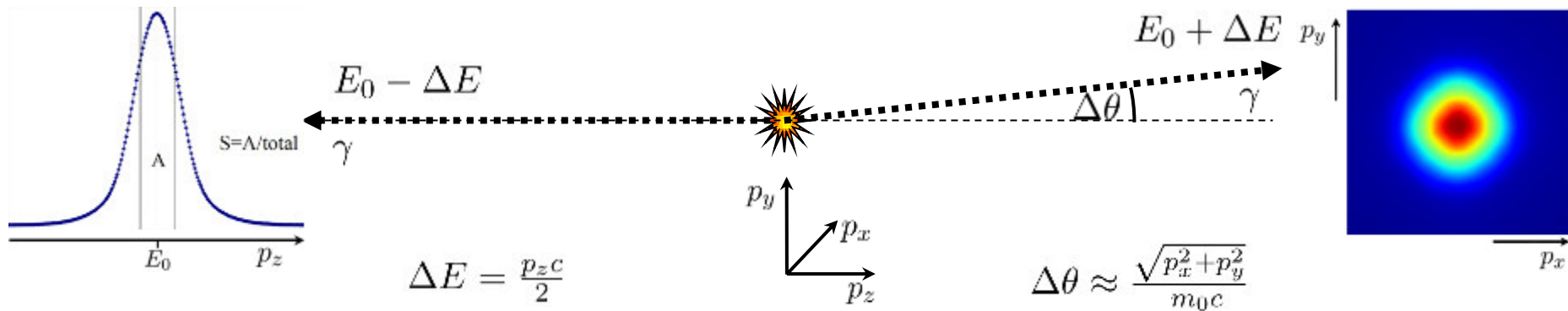


Angular Correlation of Annihilation Radiation – ACAR



Coincident Doppler-Broadening Spectroscopy – CDBS

2 γ - Annihilation & Electron Momentum



Observable

Doppler shifted γ *energy*

angle between γ 's

Detector

high *energy* resolution

high *spatial* resolution

Method

(C)DBS

2D-ACAR

e⁺ Source

NEPOMUC e⁺ beam

β^+ source ²²Na

e⁺ State

localized

delocalized

Physics

defect spectroscopy & imaging

electronic structure, Fermi-surface

Lab



Money



Outline

Positrons in Matter

Part I

(C)DBS at NEPOMUC

YBCO

AlCu6Mn

Part II

2D-ACAR with ^{22}Na

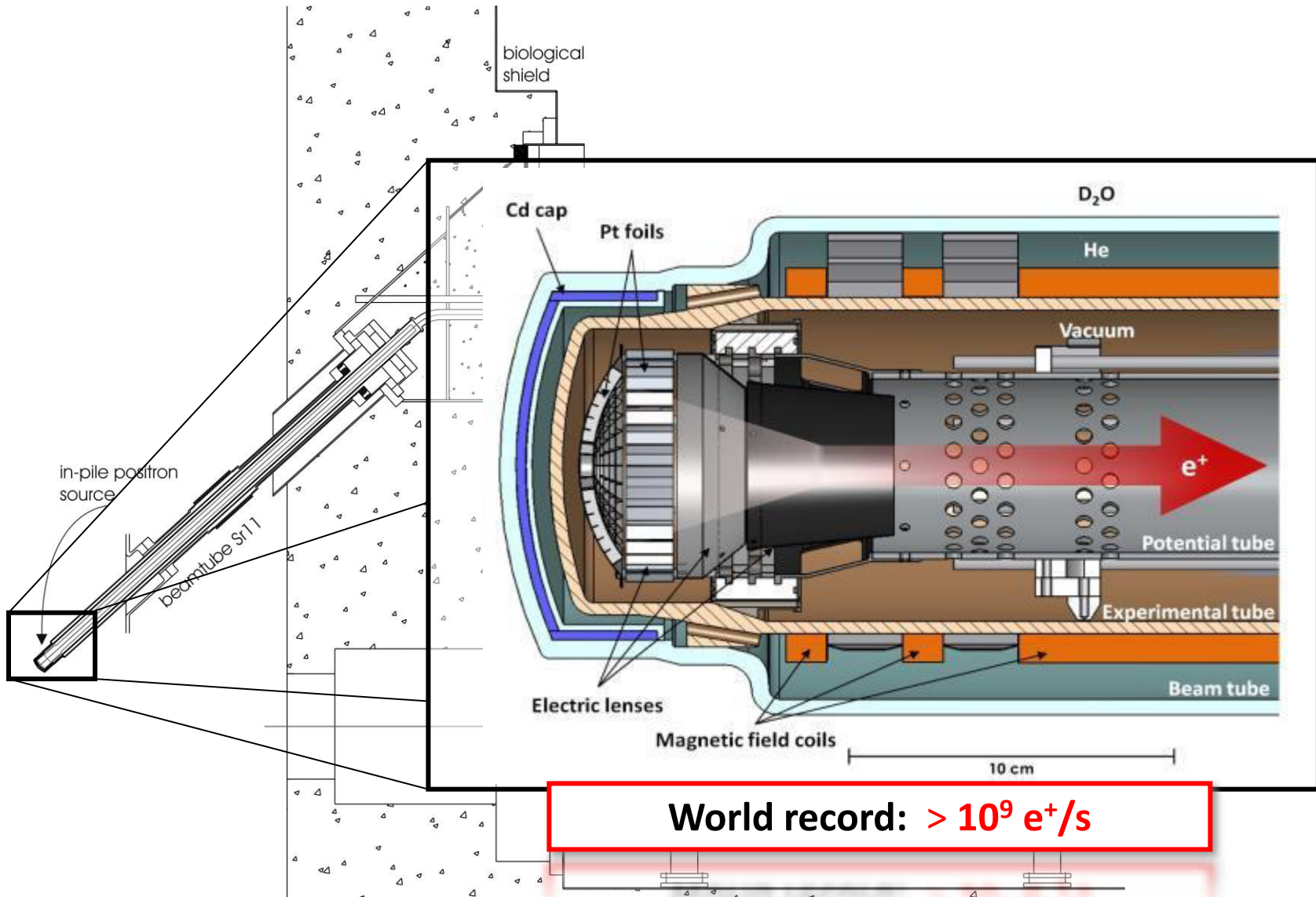
Ni

Cu_2MnAl

Conclusion & Future

NEPOMUC

NEutron induced POsitrone Source MUnich



C. H. et al NIM A 593 (2008) 616; New J. Phys. 14 (2012) 055027; J. Phys. Conf. Ser. 443 (2013) 012079; Surf. Sci. Reports 71 (2016) 547

Positron Beam at NEPOMUC

■ Pair production in Pt

$$\gamma \rightarrow e^+ e^-$$

■ Pt as converter **AND** moderator

$$\phi_{\text{Pt}}^+ = -1.95(5) \text{ eV}$$

$$E_{e^+} \sim \text{keV}$$

$$\Delta E < 2 \text{ eV}$$

■ Primary beam

Remoderated beam

E **1 keV**

20 eV

d_{FWHM} **9 mm @5 mT**

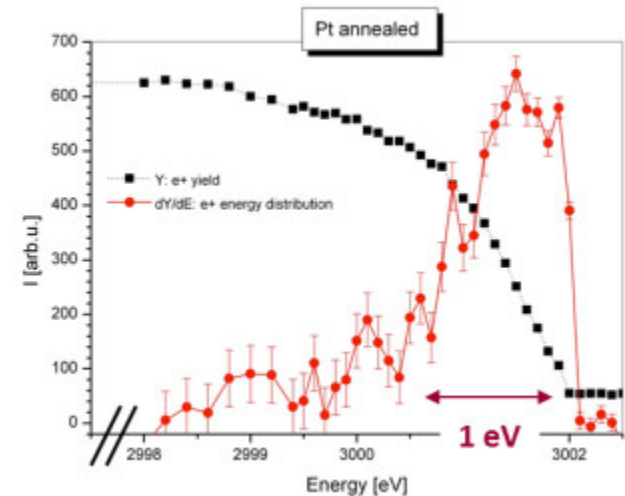
< 2 mm @4 mT

I_{beam} **$1.1 \cdot 10^9 \text{ e}^+/\text{s}$**

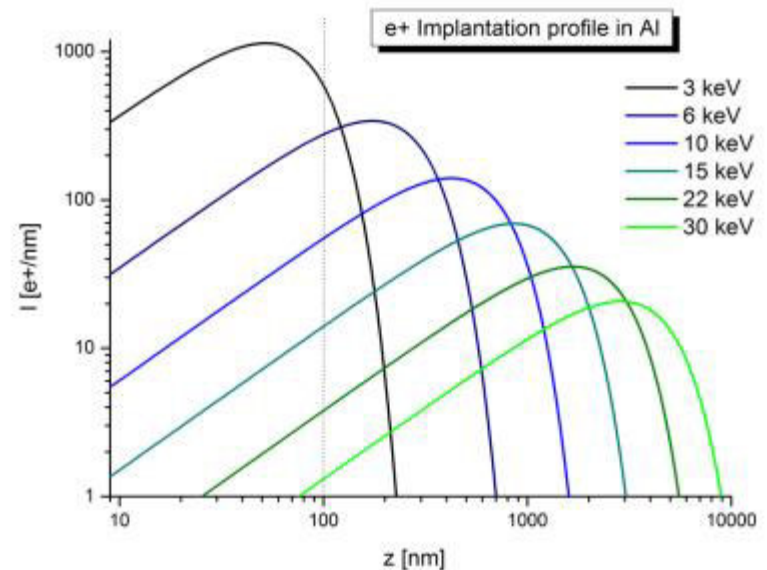
$4\text{-}5 \cdot 10^7 \text{ e}^+/\text{s}$

■ CDBS: Acceleration at sample

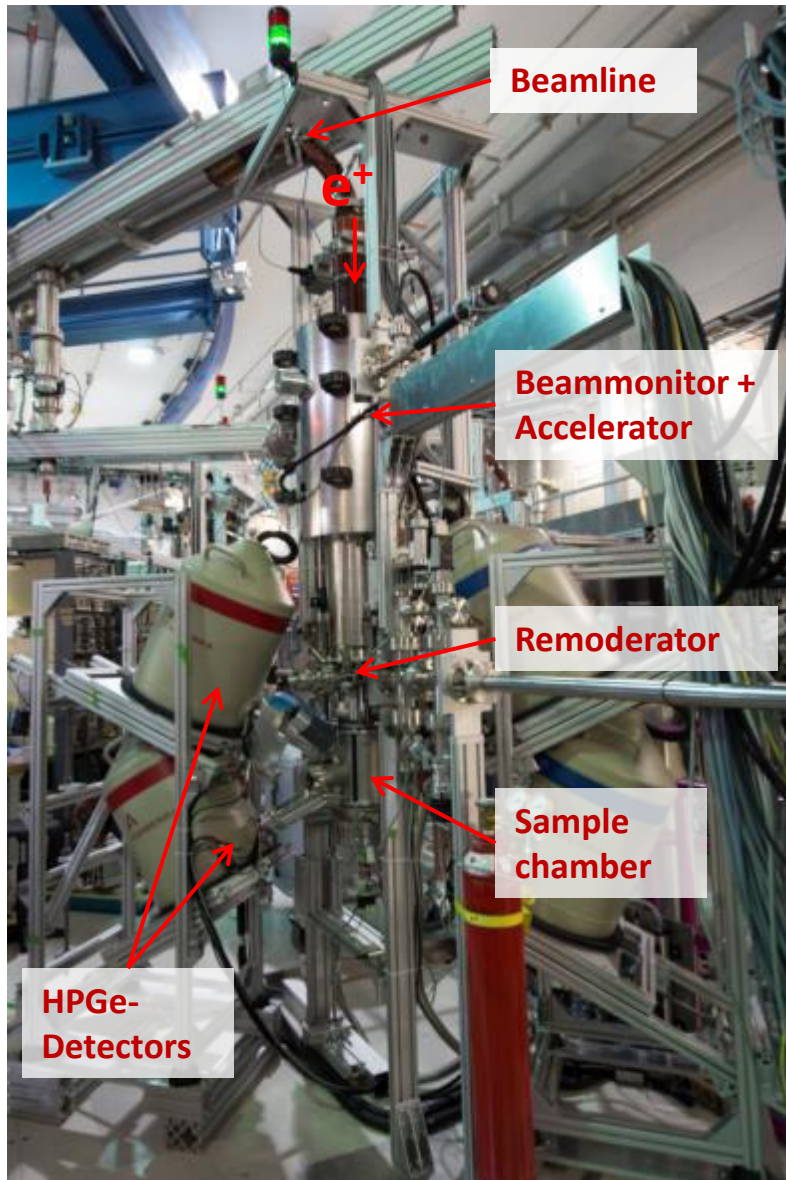
$$E = 0.1 - 30 \text{ keV}$$



C. H. et al. NIM B 198 (2002) 220

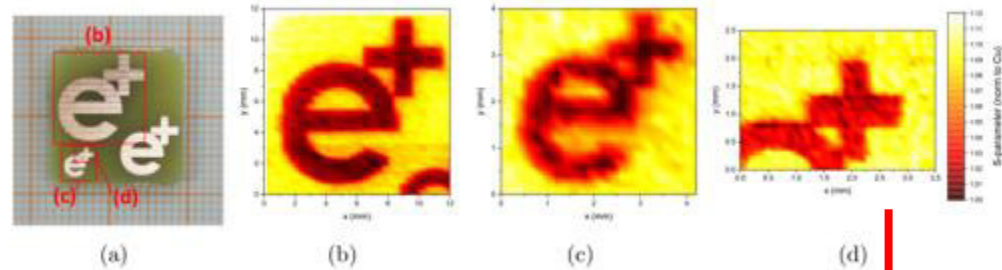
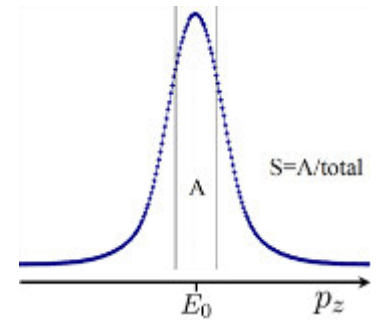


CDB Spectrometer at NEPOMUC



Doppler broadening spectroscopy:

- S-parameter: $S(T), S(E), S(x, y)$



- NEPOMUC rem. beam: 253 μm
- **CDB microbeam: 49 μm** ←
- + aperture: 33 μm
- Scan area: 19x19 mm^2

T. Gigl, L. Beddrich, M. Dickmann, B. Rienäcker, M. Thalmayr, S. Vohburger, and C. Hugenschmidt, New J. Phys. 19 (2017) 123007

Superconductivity in YBCO

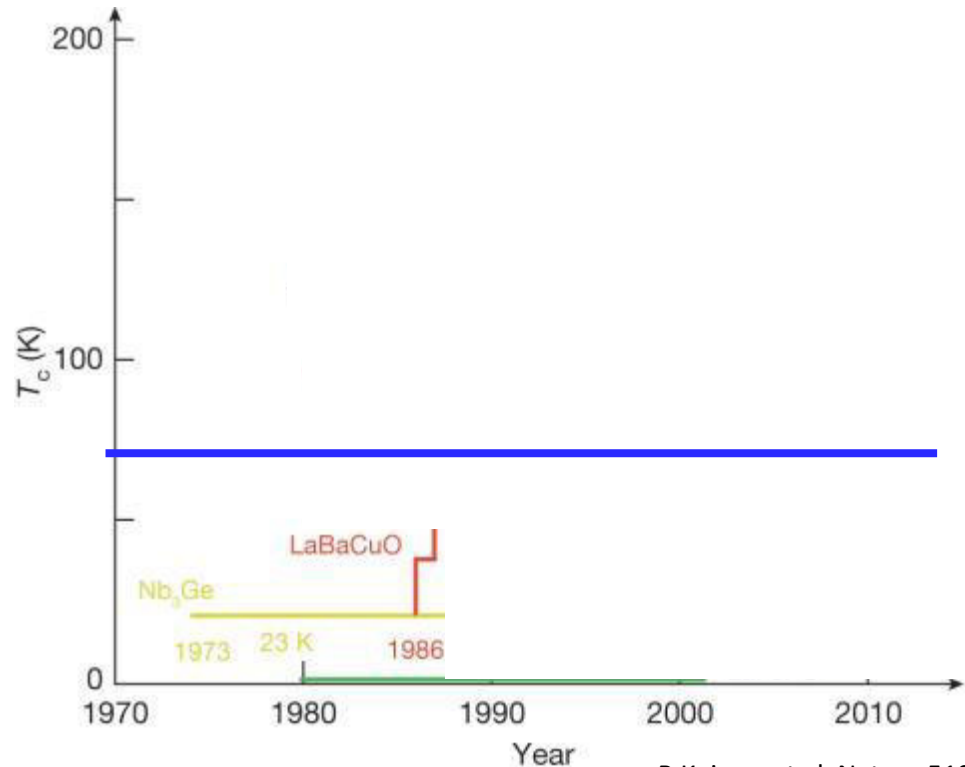
High- T_c Superconductivity in Cuprates

■ **LaBaCuO** $T_c = 35$ K

1986 A. Müller & G. Bednorz
→ 1987 Nobel prize

■ **YBa₂Cu₃O_{6.93}** $T_c = 95$ K

1987 Maw-Kuen Wu & Chu Ching-Wu



Applications of YBCO

■ **High- T_c model system**

■ **Power transmission**

■ **High field magnets**



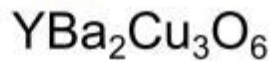
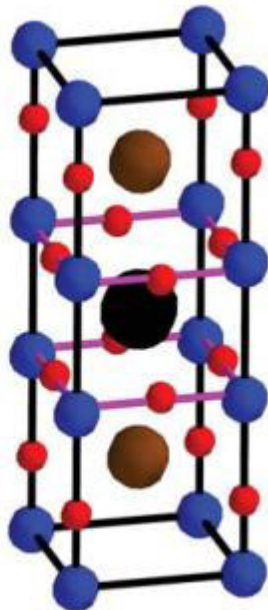
B Keimer et al. Nature 518, 179 (2015)

Superconductivity in YBCO

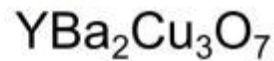
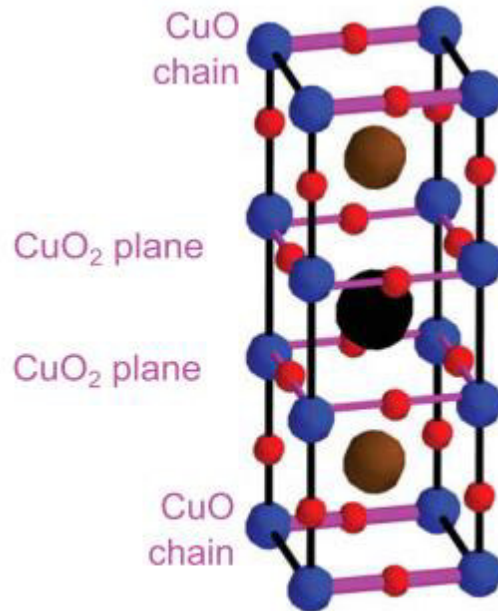
Structure

tetragonal

orthorhombic

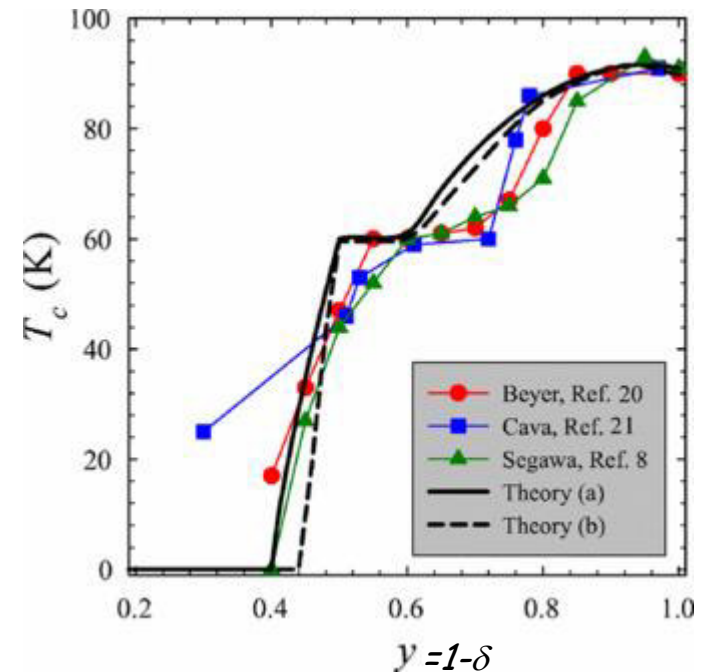


insulating



superconducting

Phase Diagram



Zaleski et al. PRB, 74 (2006) 014504

→ Oxygen content crucial for T_c

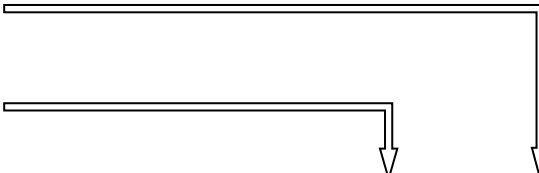
Single Crystalline $\text{YBa}_2\text{Cu}_3\text{O}_{7-\delta}$ Thin Films

Preparation

- Pulsed Laser Deposition (PLD) on STO substrate → **Thickness 210 nm +/-10 nm**
- Heat treatment ($\sim 400^\circ\text{C}$) → Reduction of oxygen content

Characterization

- Transport measurements
 - XRD → c-axis parameter
- δ and T_c *mean* values



Sample	δ	T_c (K)	t_{temp} (min)	p_{temp} (mbar)
A1	0.191	90	n. a.	n. a.
A2	0.475	60	30	$2 \cdot 10^{-2}$ (O_2)
A3	0.641	60	30	10^{-7}
A4	0.791	25	50	10^{-7}

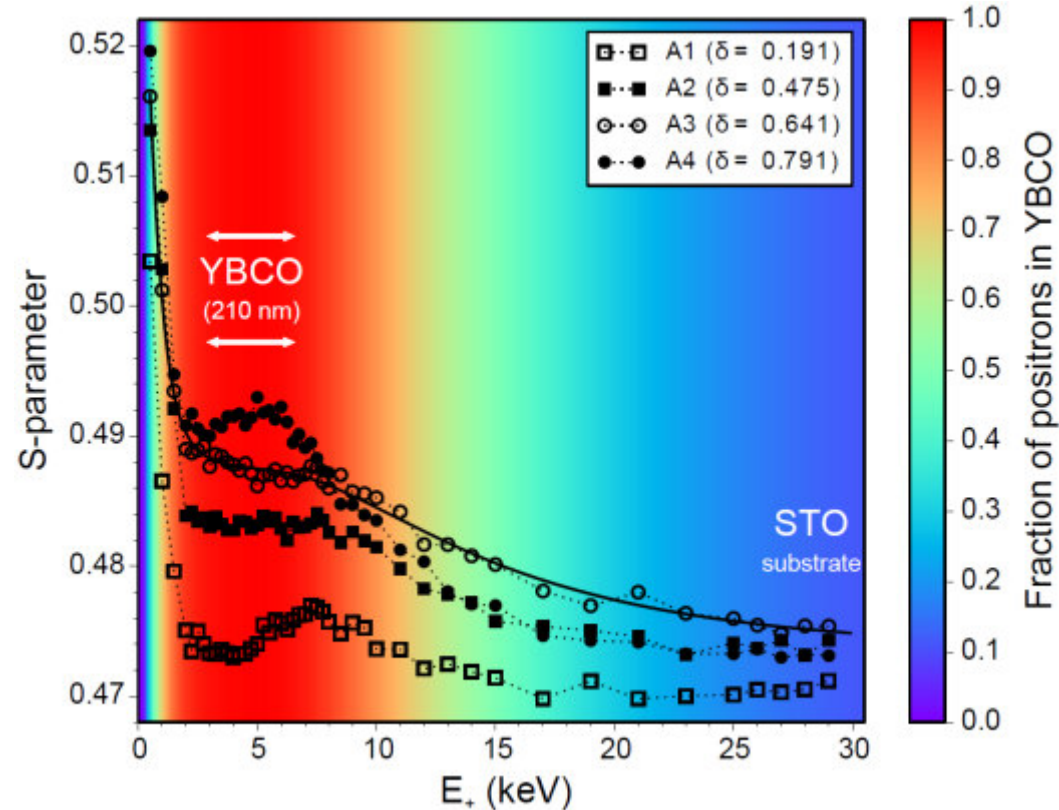
Positrons

- DBS (x,y,E,T) & CDBS
- $\delta(x,y,z)$ & $T_c(x,y,z)$

DBS on YBCO Thin Films

$S(E) \rightarrow$ depth dependent positron annihilation

- Surface: $E < 3$ keV
Steep increase of S
 \rightarrow Low positron mobility
- YBCO film: $E < 7.5$ keV
- Interface YBCO/STO: 7.5 keV



Data fit:

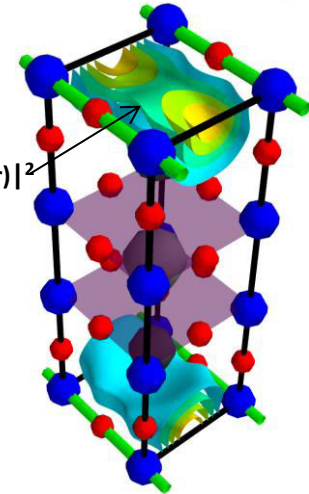
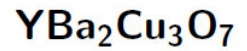
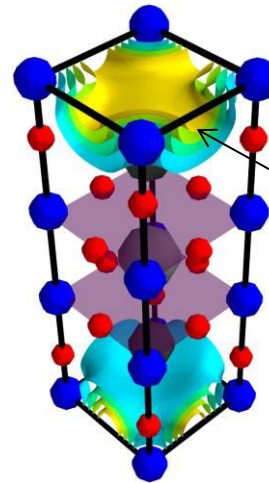
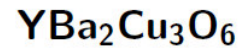
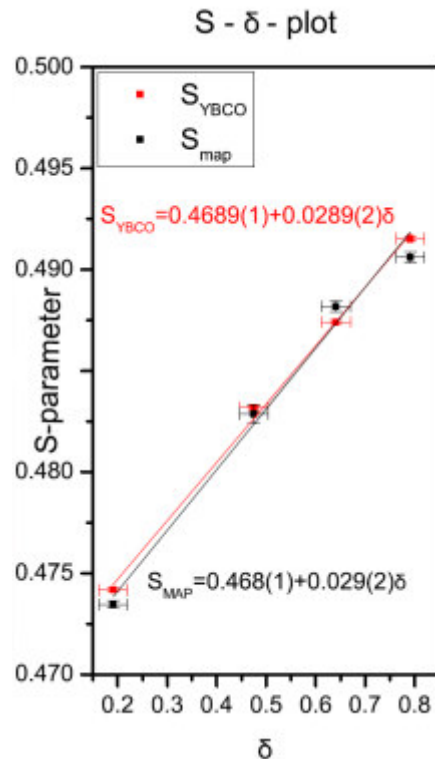
- $S(E)$ fit with a two-layer model: 210 nm YBCO on STO
 - \rightarrow Fraction of positrons annihilating in YBCO layer
 - \rightarrow Very short diffusion length: 1-2nm

Oxygen Deficiency in YBCO

Positrons in $\text{YBa}_2\text{Cu}_3\text{O}_{7-\delta}$

- Positrons probe plane of oxygen deficiency
- Low positron mobility along c-axis
→ as observed in $S(E)$

- Linear correlation of δ (XRD) with S (DBS):

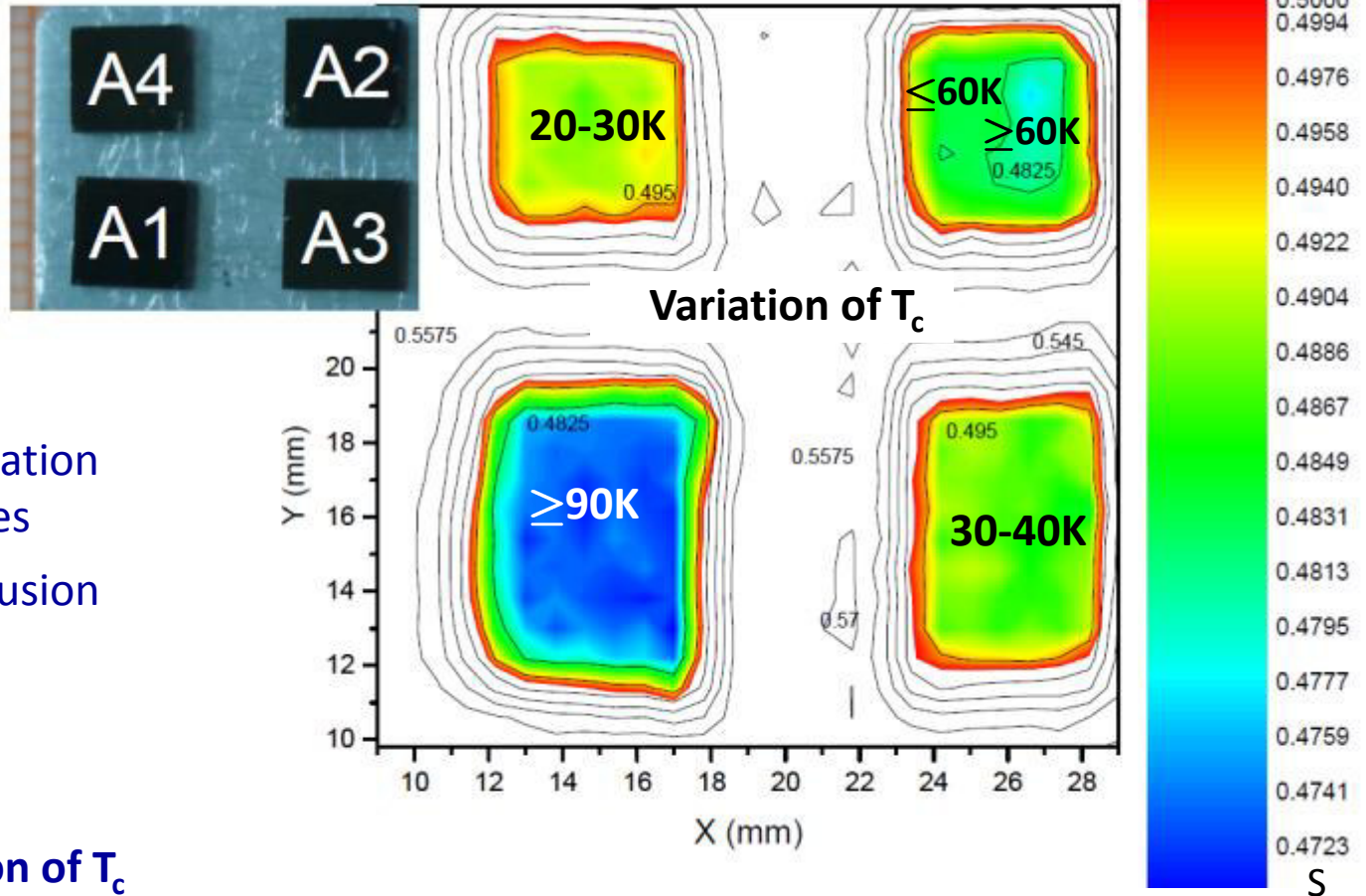


DBS with Positronbeam

- $\text{YBa}_2\text{Cu}_3\text{O}_{7-\delta}$: Measure spatial distribution of δ and determine local variation of T_c

Imaging of δ and T_c Variation

DBS with Scanning Positron Beam $\rightarrow S(x,y)$



■ $S(\delta)$:

\rightarrow Spatial δ variation within samples

\rightarrow Local out diffusion of oxygen

■ $T_c(\delta)$:

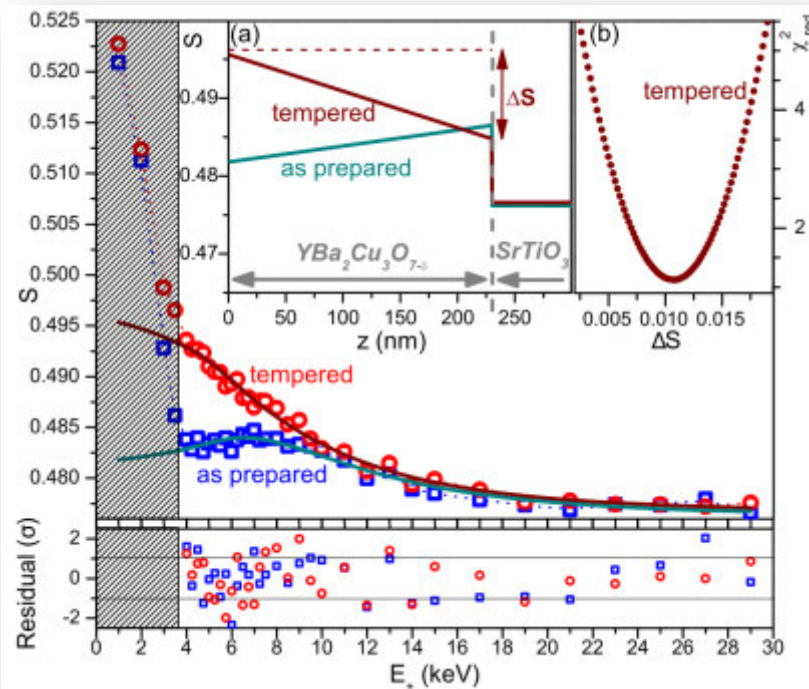
\rightarrow Local variation of T_c

Depth Profile of T_c

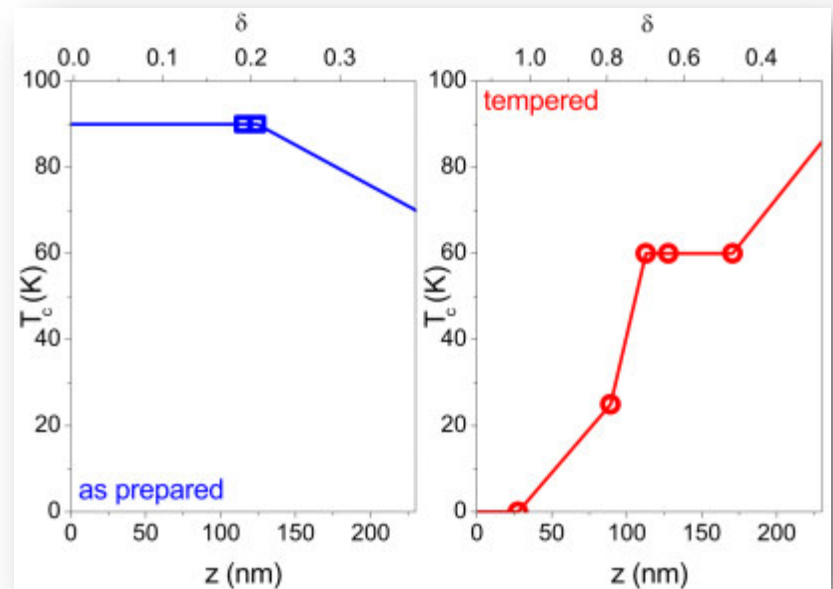
DBS with Positron Beam $\rightarrow S(z)$

- 230nm YBCO film as prepared & after tempering at 400°C
- Use simple model for $S(z)$ sufficient to explain $S(E_+)$

$S(E_+) \rightarrow S(z)$



$\delta(z) \rightarrow T_c(z)$



(dots: ref. samples)

Laser Beam Welded Al Alloy

Material: AlCu6Mn (EN AW 2219-T87)

- Age hardenable Al alloy
- High strength and low weight

Laser beam welding: (LBW)

- Beam spot & heat impact small
→ small heat affected zone (HAZ)
- Weld accuracy & reproducibility high

LBW of Al alloys:

- Weight reduction
→ replacement of steel and riveted joints

Sample preparation IWB at TUM :

- Single-mode laser (IPG YLR-3000)
- Laser power: 2.6 kW
- Spot size: 50 μm
Oscillating with 200 Hz, 0.2 mm amplitude
- Welding speed: 100 mm/s.

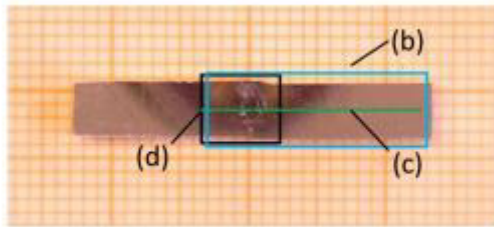


To be studied:

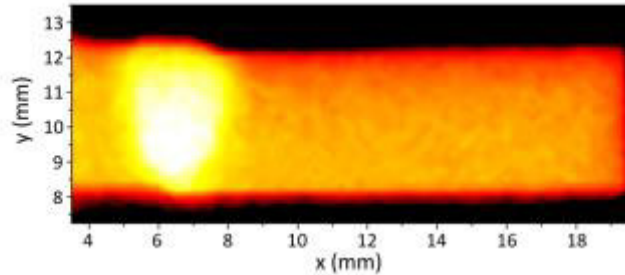
- Improvement of mechanical stability of joint
- What about (point) defects?
- Spatial distribution of precipitates?

Defect Mapping on a LBW

Sample: Laser beam weld (LBW) of **AlCu6Mn** (EN AW 2219-T87)

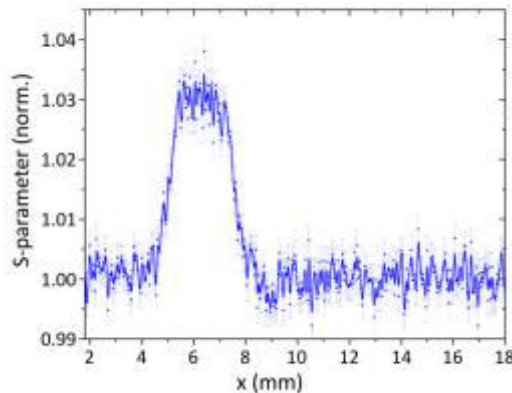


(a)



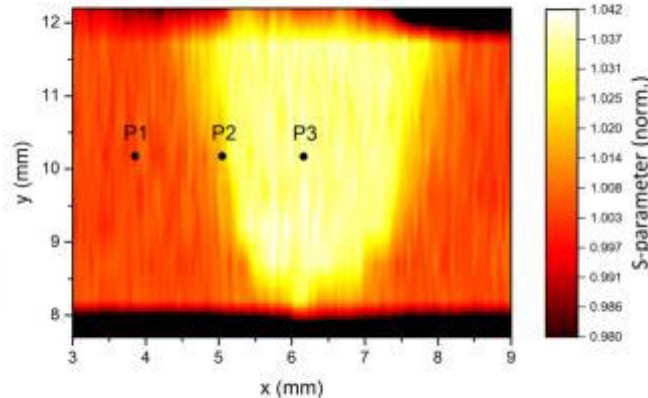
(b)

NEPOMUC rem. Beam
Overview **2D map**
 $\Delta x, y = 200 \mu\text{m}$



(c)

Positron microbeam
High resolution **line scan**
 $y = 10 \text{ mm}$, $\Delta x = 50 \mu\text{m}$

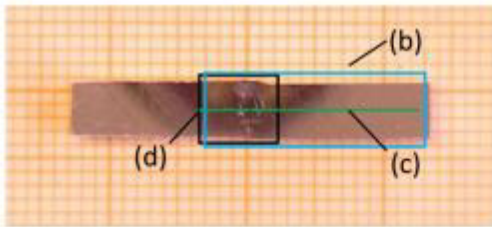


(d)

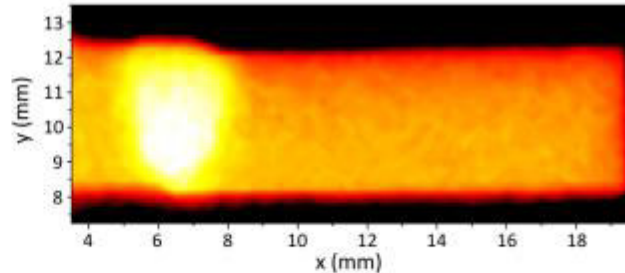
Positron microbeam
High resolution **2D map**
 $\Delta x = 50 \mu\text{m}$, $\Delta y = 500 \mu\text{m}$

Defect Mapping on a LBW

Results:

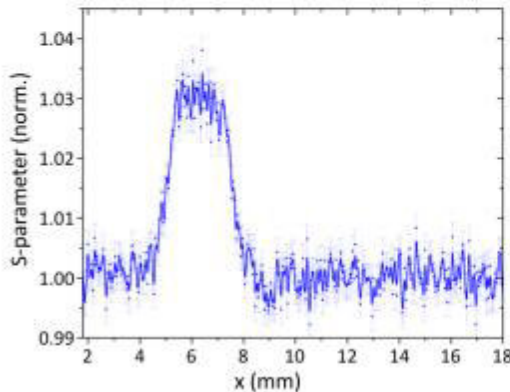


(a)



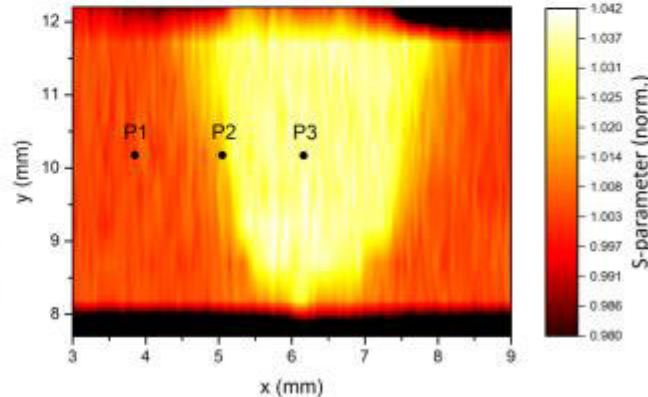
(b)

Gradient of $S(y)$ outside LBW
→ defect gradient generated during **cold-rolling**



(c)

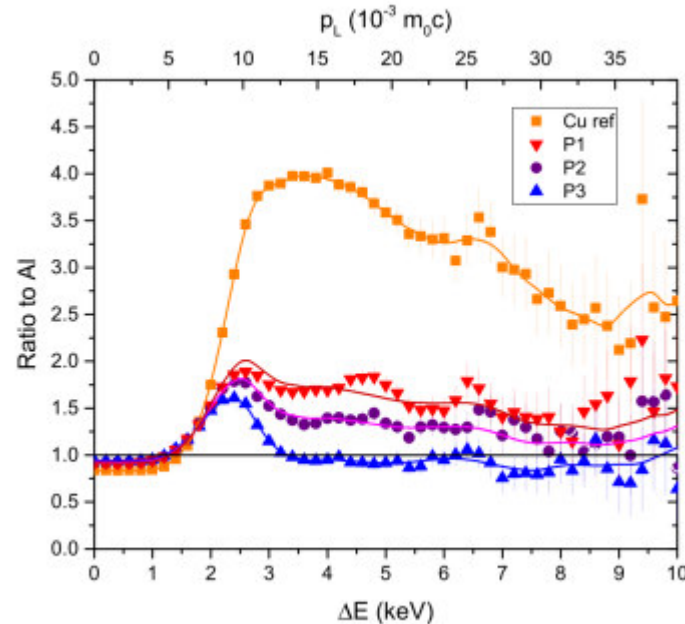
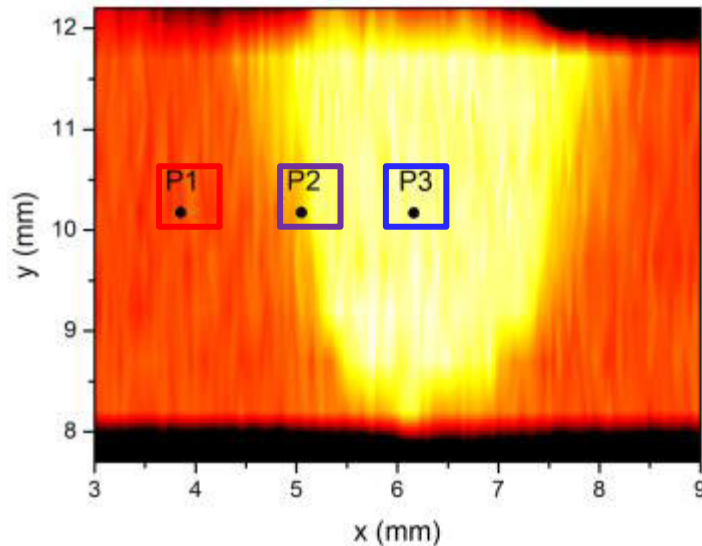
Sharp transition at LBW edges
→ well localized **small** heat affected zone (**HAZ**)



(d)

Drastic increase of S in LBW
→ creation and quenching of a large amount of **vacancy-like defects**

CDBS at LBW of AlCu6Mn



P1, P2

- Significant contribution of Cu signature
→ positron trapping at **Cu rich precipitates**;
in agreement with artificially age-hardened precipitates (Θ phase, Al_2Cu phase)

P3

- Disappearance of Cu signature
→ melting of Cu rich phases + rapid cooling
→ formation of **supersaturated solid solution**
- Appearance of confinement peak:
→ presence of **vacancies** (& $V_{\text{Al}}\text{-Cu}$)

Conclusion: Al Alloys & YBCO

LBW of Al Alloys:

- **2D defect imaging** within short time and $<50\mu\text{m}$ resolution
- **Identification of Cu precipitates**

High T_c -Superconductors

- Positron ideal **probe for oxygen deficiency δ** in YBCO
- Non-destructive **spatial resolved determination of δ and T_c !**

Outline

Positrons in Matter

Part I

(C)DBS at NEPOMUC

YBCO

AlCu6Mn

Part II

2D-ACAR with ^{22}Na

Ni

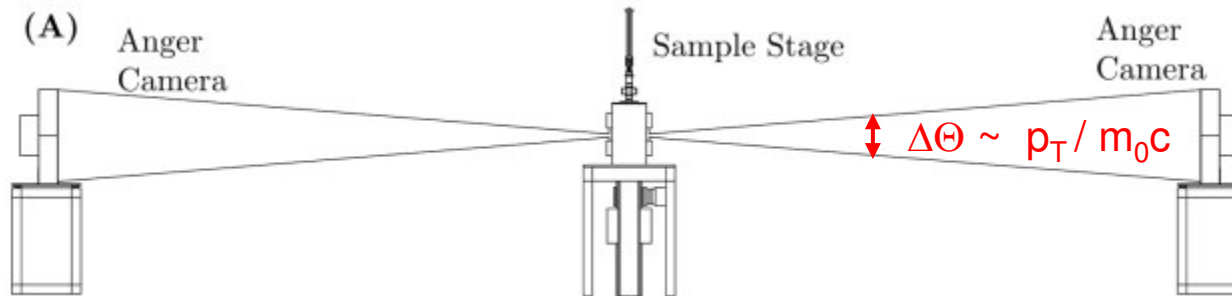
Cu_2MnAl

Conclusion & Future

ACAR

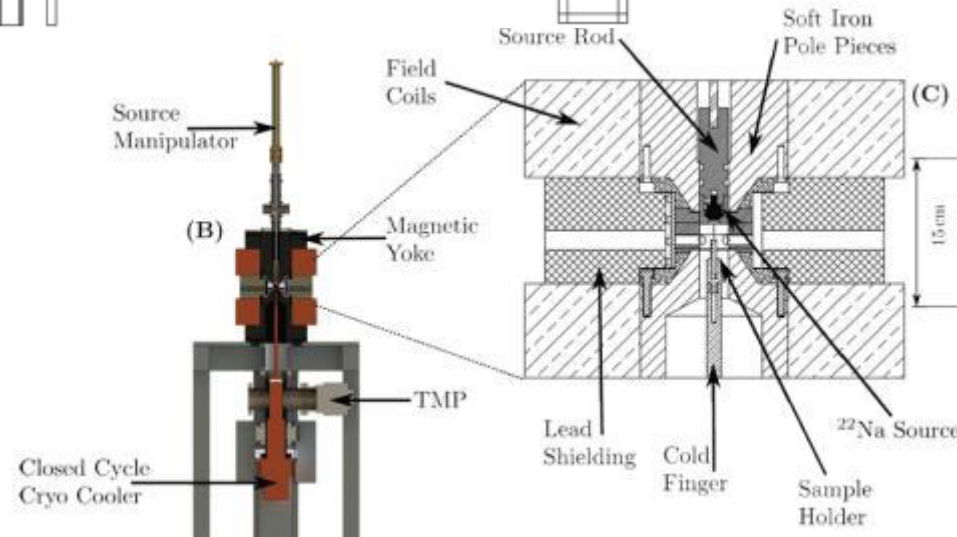
Angular Correlation of Annihilation Radiation

2D-ACAR spectrometer at TUM:



Applications & features:

- Determination of electronic structure
→ Anisotropy of Fermi Surface
- Special conditions **not** required
→ $T \gg 0$, no B-field
- β^+ source
→ spin-polarized ACAR



Ceeh et al. Rev. Sci. Instrum. 84, 043905 (2013)

Future:

- e^+ beam → surface, interface, thin layers, 2D electron systems...

2D-ACAR: Principle

Electron momentum density

$N(p_x, p_y)$: 2D projection of 3D electron momentum density

$$N(p_x, p_y) \propto \int dp_z \sum_{i=\text{occ.}} \sum_j \left| \int e^{-i\mathbf{r} \cdot \mathbf{p}} \psi^+(\mathbf{r}) \psi_{i,j}^-(\mathbf{r}) d\mathbf{r} \right|^2$$

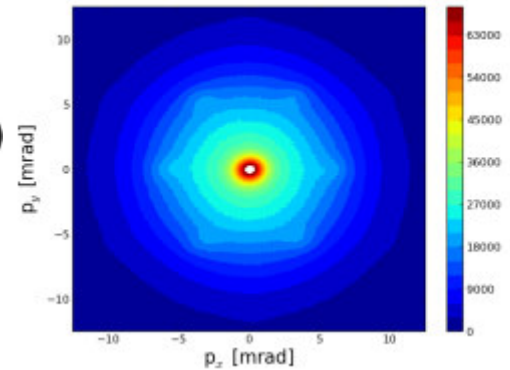
- ▶ product of positron and electron wavefunction
- ▶ in momentum space
- ▶ sum over all occupied states i in all bands j
- ▶ projecting along the longitudinal component

2D-ACAR: Principle

- 2D-ACAR spectrum:

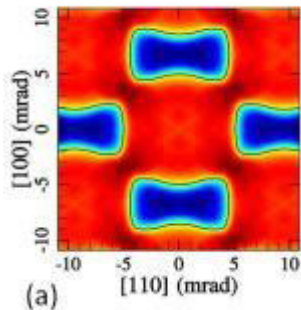
$$N(\theta, \phi) = N(p_x, p_y) = \left(\int \rho^{2\gamma}(\mathbf{p}) dp_z \right) \otimes R(p_x, p_y)$$

- Backfolding into first Brillouin zone

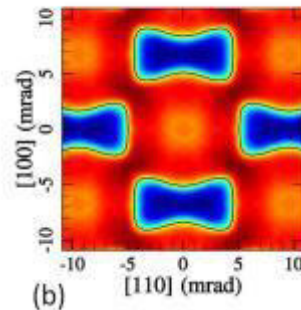


- 3D-reconstruction of FS from 2D-projections
- 2D-Cuts through FS

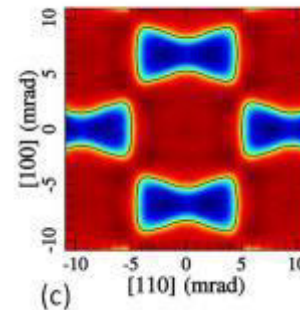
Example: FS of Cu at low T and RT



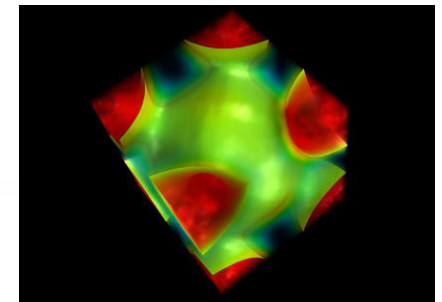
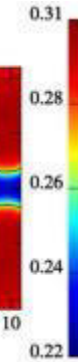
10K



300K



300K (from 2D proj.)

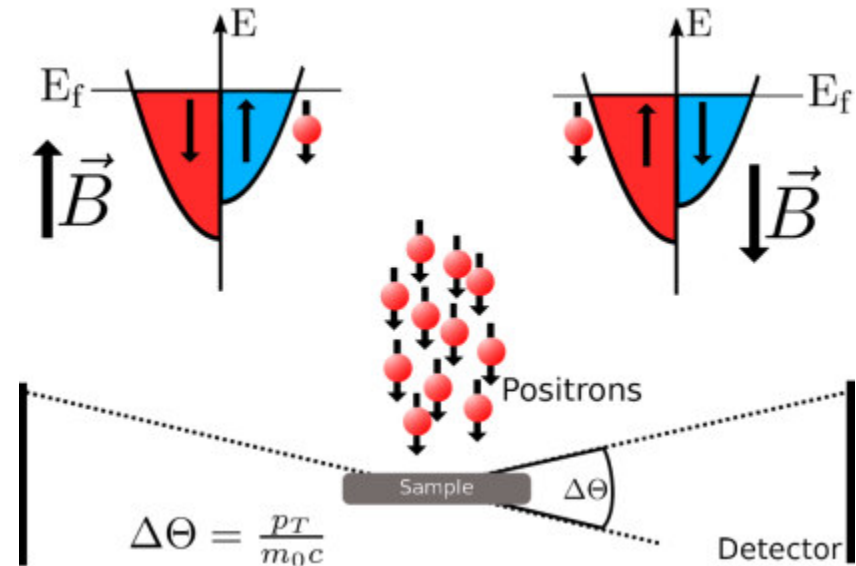


J. A. Weber et al.
J. Phys. Conf. Ser., 443(2013) 012092

Comparison with theory

Spin-Polarized ACAR

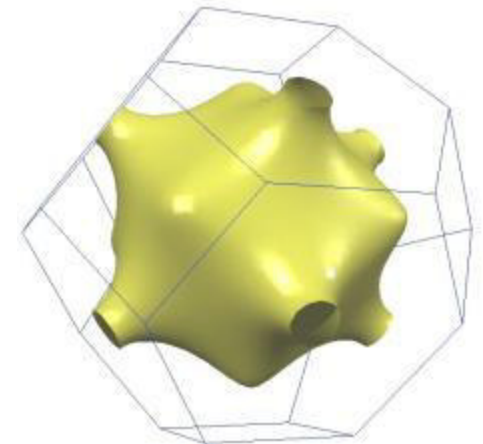
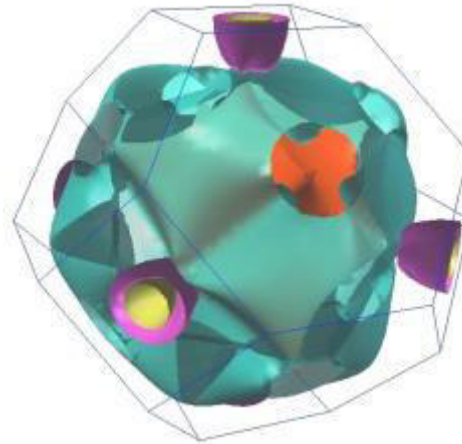
- Beta-decay \rightarrow right-handed positrons
- Singlet 2γ -annihilation strongly favored
- Change magnetization of the sample
 \rightarrow positron predominantly probes either of the two spin bands
- Look at difference spectrum $\uparrow - \downarrow$: $N_{\pm}(p_x, p_y)$



Electron Correlations in Nickel

Nickel

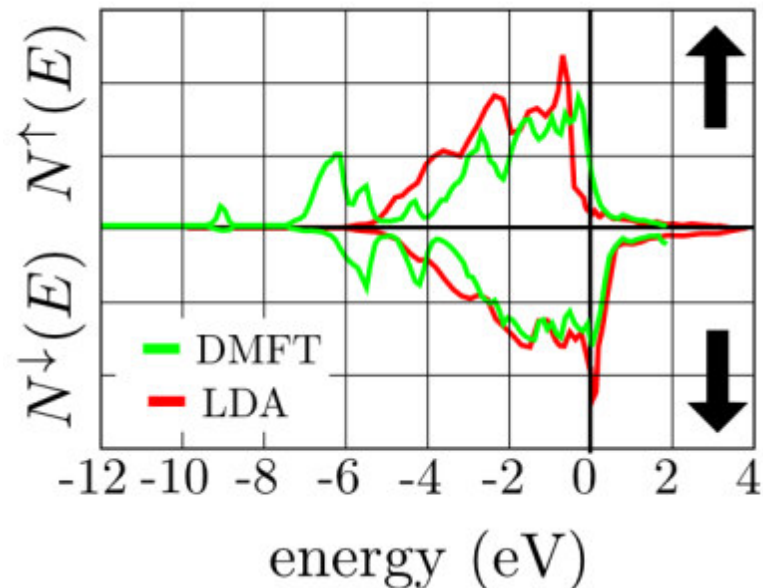
- Magnetic FCC metal
- One unpaired 3d-electron
- "simple" test case for theory and experiment



<http://www.phys.u.edu>

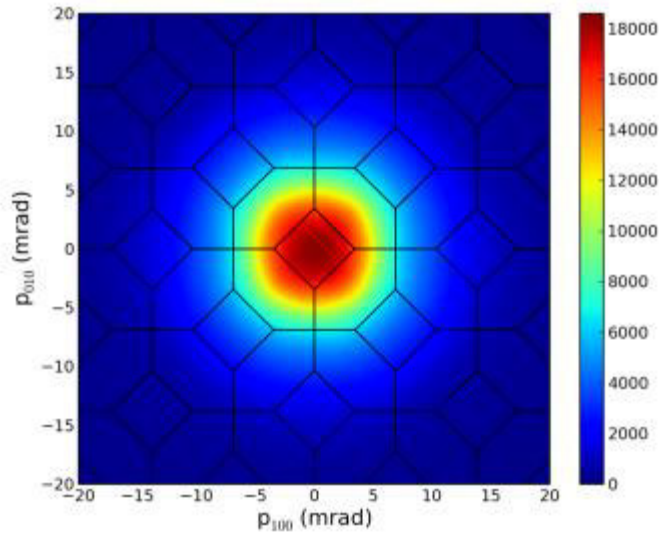
Theory

- 6eV satellite peak arises when correlations are included (DMFT)
- Electron states are relocated
- Effect of correlation change the appearance of the Fermi surface

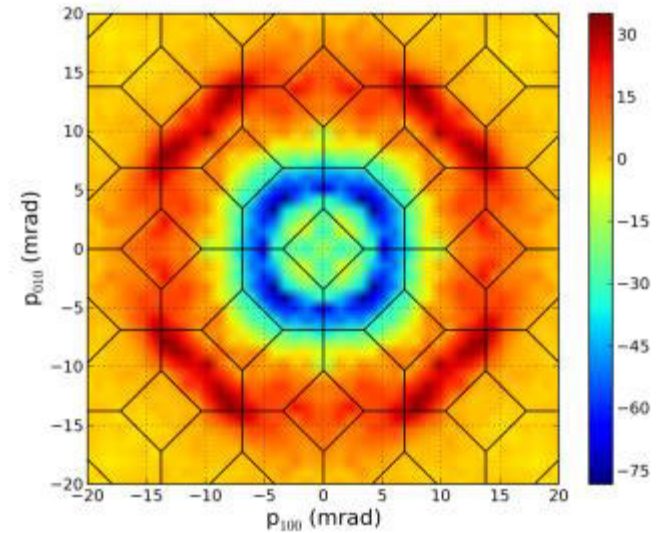


Nickel: 2D-ACAR Results

Raw spectrum

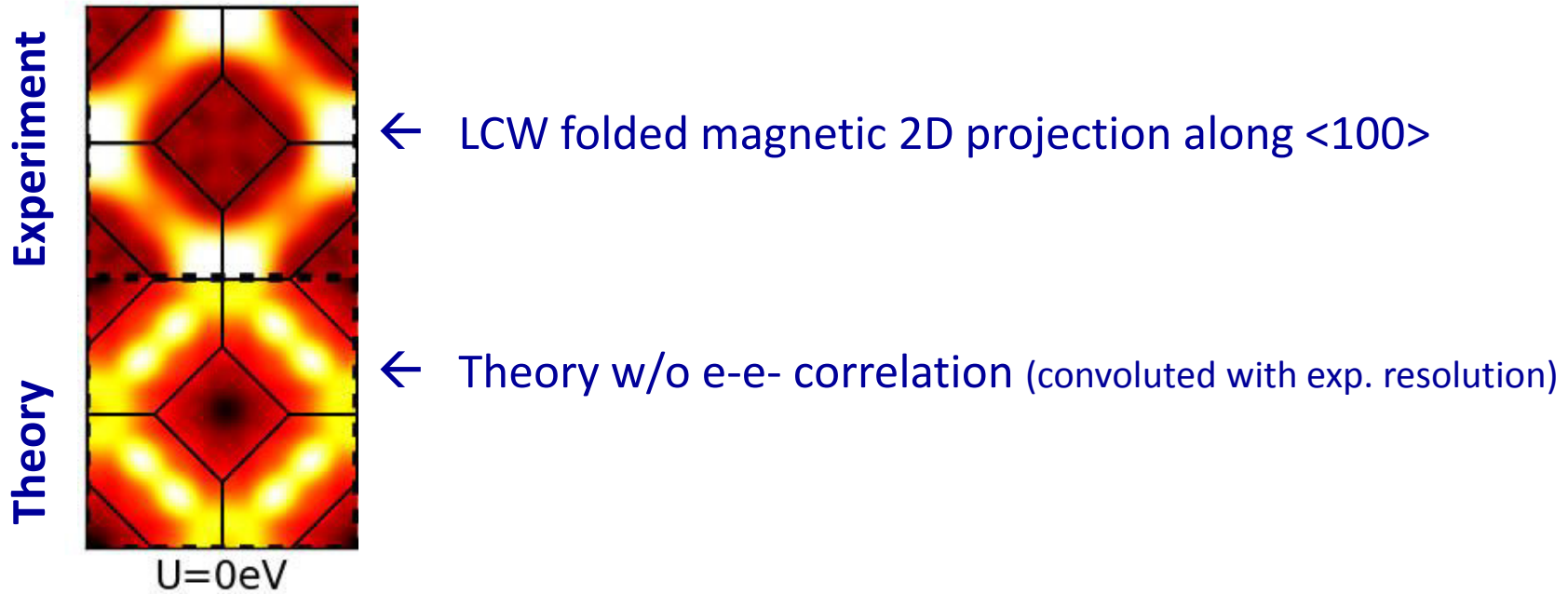


Difference



- Integration direction along $\langle 100 \rangle$: 4-fold symmetry
- Magnetic difference spectrum exhibits the same symmetry

Nickel: Comparison with Theory

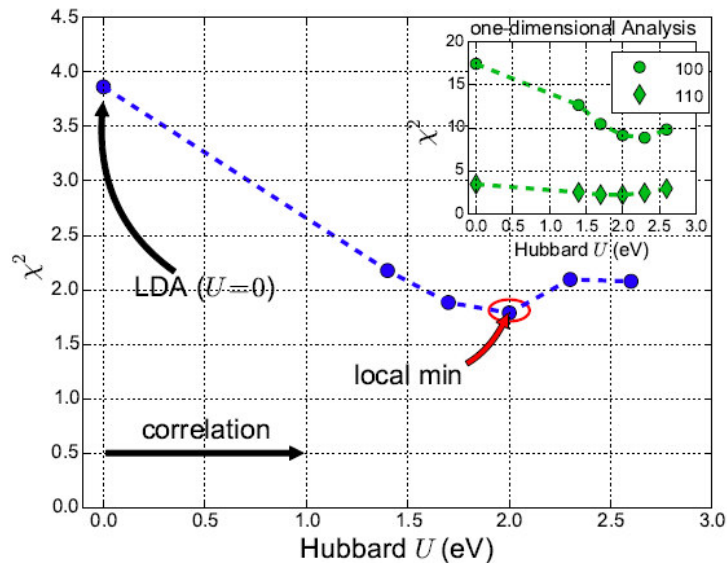
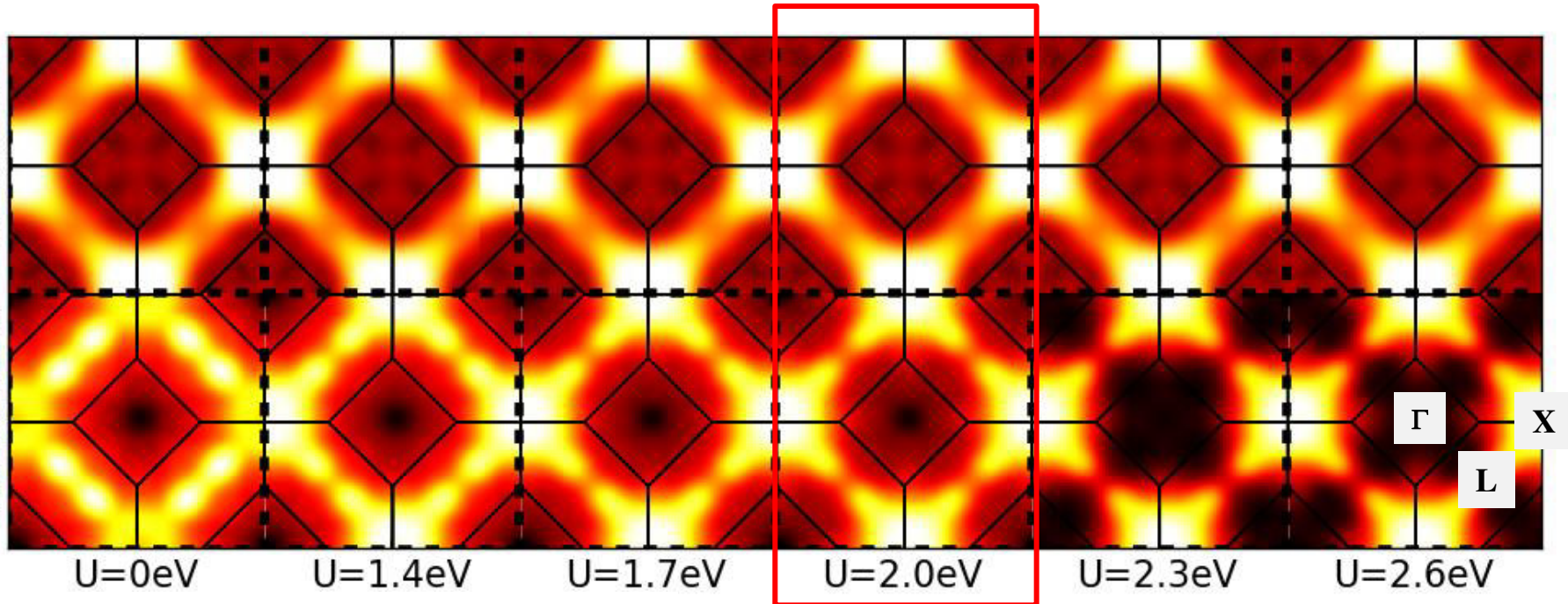


■ Significant effect due to electronic correlations

Electron Correlation Strength in Nickel

Experiment

Theory



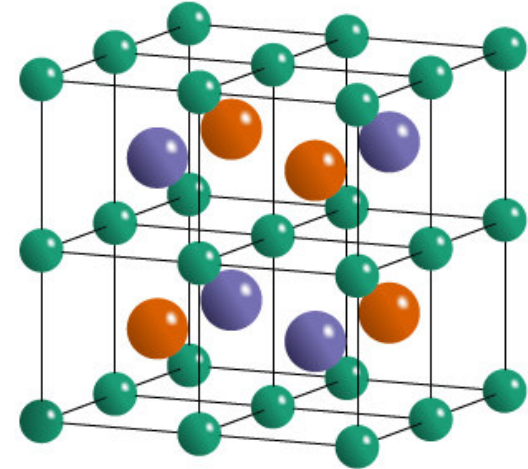
Effect of correlations in Nickel

- Electron-electron correlation strength:
 $U = 2.0(1) \text{ eV}$
- d -bands pushed below the Fermi level

Electronic Structure of Cu_2MnAl

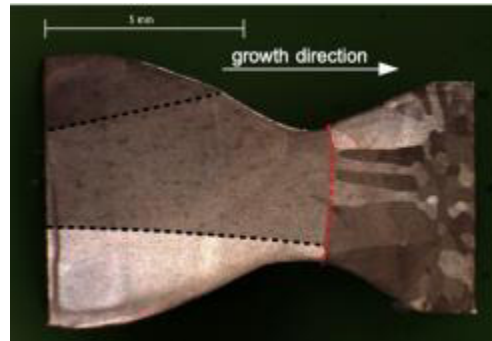
Heusler compounds

- F. Heusler 1903: ferromagnetic Cu_2MnAl
- Formula X_2YZ (Space group $L2_1$)
 - X, Y transition metals
 - Z non-magnetic/non-metallic element
- Large variety of electronic ground states:
 - Insulating, (half-)metallic, semiconducting, ferromagnetic, superconducting

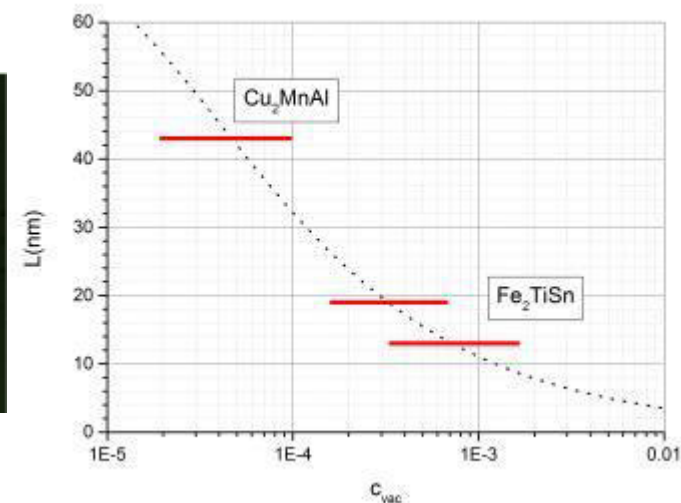


Single crystalline Cu_2MnAl

- Demanding to produce “large” & defect free samples
 - Samples grown by optical floating zone
- A. Neubauer, A. Bauer, C. Pfleiderer



A. Neubauer et al. NIM A 688 (2012) 66

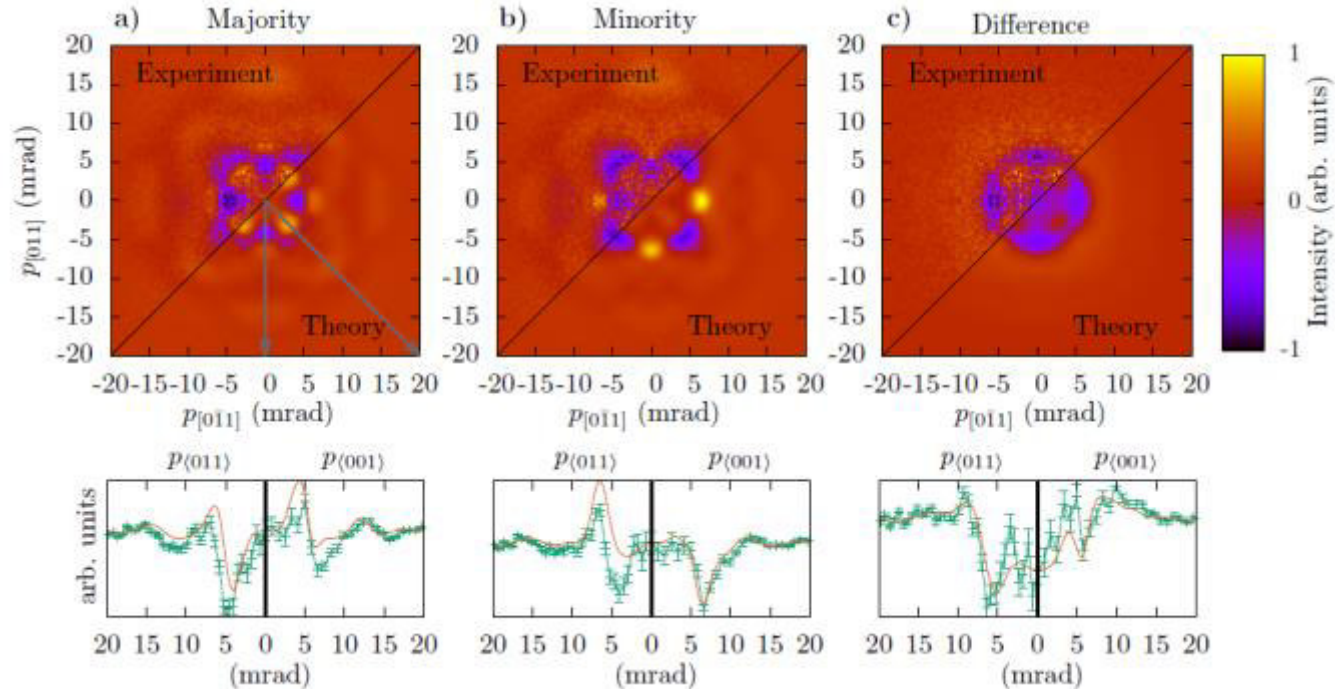


C.H. et al. Appl. Phys. A 119 (2015) 997

Spin-Polarized 2D-ACAR on Cu_2MnAl

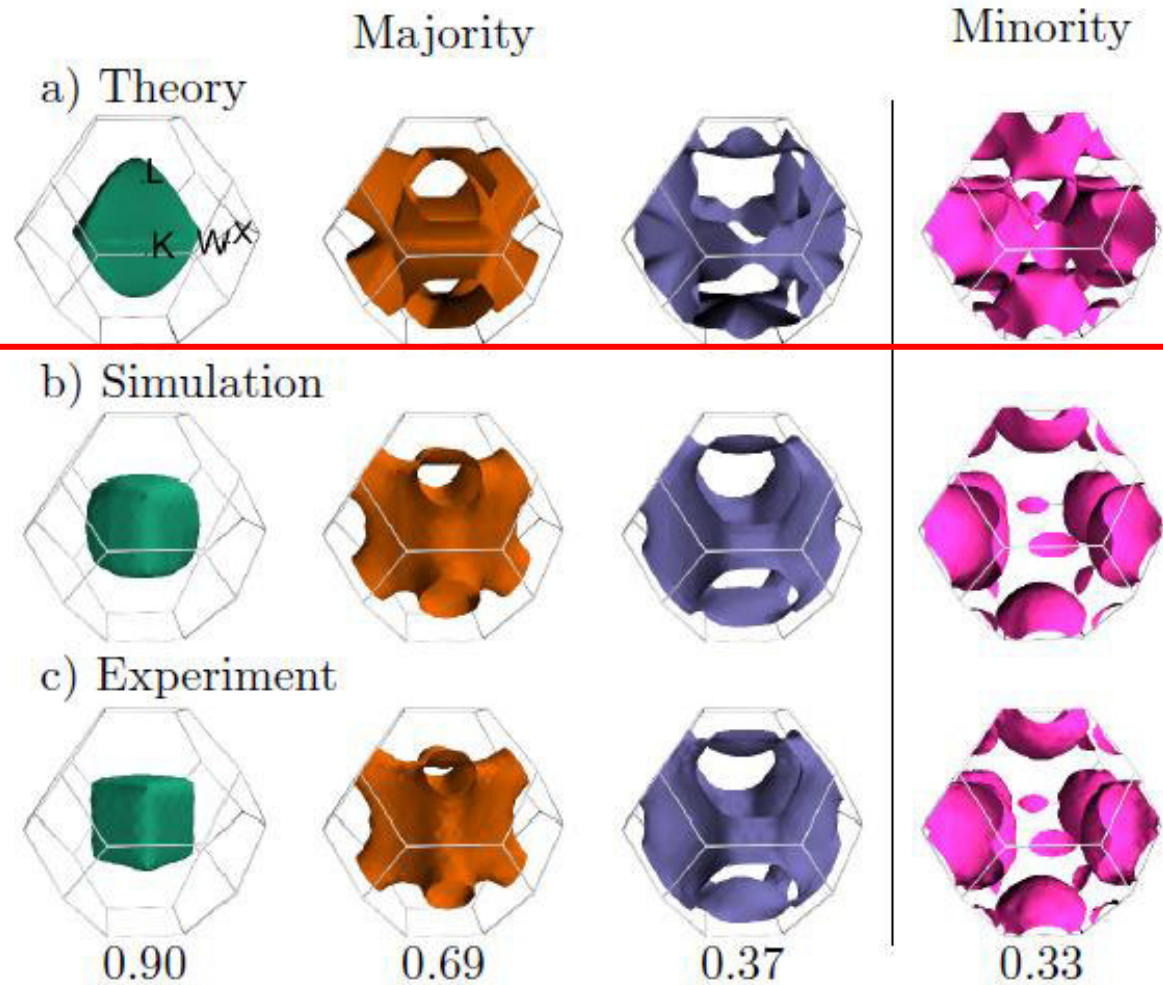
Cu_2MnAl

2D projections along [100] at RT \rightarrow anisotropy of maj., min. density & difference



- Excellent agreement between theory and experiment
 \rightarrow 3D reconstruction of Fermi sheets for individual spin channels

Cu₂MnAl: 3D Reconstruction of Fermi Surface



Results

■ Contribution of each individual Fermi sheet to magnetization !

■ Total magnetization: 3.6(5) $\mu\text{B}/\text{f.u.}$

Summary

- World-class positron beam at NEPOMUC

→ fundamental research

What about *- spin-polarized -*

even higher intensity?

- CDBS with scanning probe

→ spectroscopy and imaging of **defects**

- Spin-resolved 2D-ACAR for electronic structure determination

Evolution of the FS *- spin-resolved -*

from the surface to the bulk

- Experiment

→ Determination of **correlation strength** in Ni

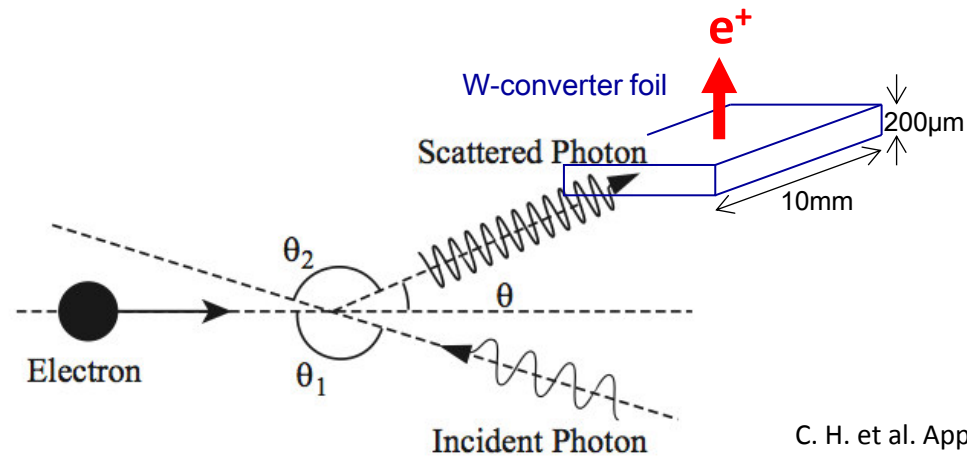
→ Revealing **spin-resolved Fermi sheets** in Cu_2MnAl

Plans for a Next-Generation Positron Beam



Inverse Compton Scattering & Positron Production

$$v_{sc} \sim \gamma^2 v_0$$
$$\rightarrow \gamma \sim 1000$$



C. H. et al. Appl. Phys. B 106 (2012) 241

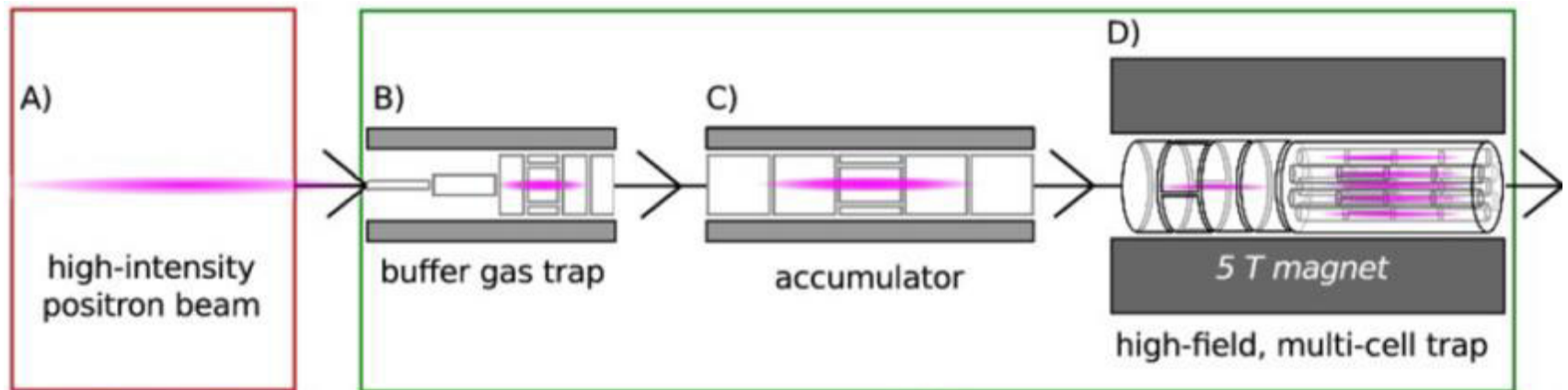
Features:

- Tiny diameter of γ beam \rightarrow **high brightness**
- Narrow band width \rightarrow no γ 's with $E < 2mc^2$
- **Polarization** \rightarrow spin-resolved positron beam experiments

ELI-NP positron source project:

- Flux of moderated positrons: $1-2 \cdot 10^6$ e+/s
- Degree of polarization: 31-45%

Ultra-Dense Positron Pulses



- A) **NEPOMUC:** continuous positron beam (primary or remoderated)
- B) **Cooling & trapping** in buffer gas trap
- C) **Accumulation** in UHV
- D) **Collection** and accumulation in multi-cell trap

■ **Aim: Pulse of 10^9 e+ within few ns**

DFG TUM/IPP (HU 978/15-1)

DFG Uni Greifswald/IPP/TUM (HU 978/16-1)

ERC advanced grant, T. Pedersen, IPP: "Pair plasma"

NEPOMUC FRM II & Physics Department TUM

Alumni: K. Schreckenbach C. Piochacz B. Straßer M. Stadlbauer J. Mayer P. Pikart M. Reiner N. Qi H. Ceeh
J. Weber S. Zimnik | S. Legl T. Brunner B. Löwe F. Lippert N. Grill M. Thalmayr G. Zagler | K. Hain M. Rutzinger
E. Erdnüss S. Sailer C. Herold M. Schleuder L. Beddrich B. Kalis ...



UniBW München

G. Dollinger, W. Egger, J. Mitteneder

**Uni Augsburg
Univ Bristol**

L. Chioncel, G. Hammerl, D. Vollhardt
S. Dugdale

TUM E21/E51

P. Böni, C. Pfeiffer

MPI Stuttgart

E. Benckiser

MLZ FRMII

W. Petry

TUM iwb

A. Bachmann

Uni Halle

R. Krause-Rehberg, R. Scheer

Univ Tsukuba

A. Uedono

Chiba Univ

M. Fujinami

Univ Tokyo/KEK

T. Hyodo, K. Wada

Univ Trento

R. Brusa

M. Doser

T. Pedersen, H. Saitoh,

J. Stanja, U. Hergenahn

L. Schweikhart

C. Surko, J. Danielson

Uni Greifswald

UCSD

M. R. Stoneking

Lawrence Univ

THANK YOU !

Deutsche
Forschungsgemeinschaft

DFG



Universität
Bayern e.V.



GEFÖRDERT VOM



Bundesministerium
für Bildung
und Forschung